Charles University

Faculty of Science

Study programme: Analytical Chemistry

Mgr. Sofiia Tvorynska

Electrochemical biosensors with spatially separated enzymatic and detection parts for selective analysis in flow-through arrangement

Elektrochemické biosenzory s prostorově oddělenou enzymatickou a detekční části pro selektivní analýzu v průtokovém uspořádání

Ph.D. Thesis

Supervisor: Prof. RNDr. Jiří Barek, CSc.

Supervisor-consultant: Bohdan Josypčuk, Ph.D.

Prague 2023

Declaration

I hereby declare that I have composed this written doctoral thesis entirely independently. I declare that all the results used and published in this Ph.D. thesis were obtained from my own experimental work and that all the ideas taken from the work of others are properly referred to in the text and the literature survey. I have not used any sources or aids other than those specified. I am conscious that the prospective use of the results published in this Ph.D. thesis outside Charles University in Prague is possible only with the written consent of Charles University.

I also declare that neither this Ph.D. thesis nor its significant part has been submitted in any form for another or the same academic degree at any university or other institution of tertiary education.

Prohlášení

Prohlašuji, že jsem tuto disertační práci zpracovala zcela samostatně. Prohlašuji, že všechny výsledky použité a publikované v této disertační práci byly získány z mé vlastní experimentální práce a že jsem uvedla všechny použité informační zdroje a literaturu. Nepoužila jsem žádné jiné zdroje nebo pomůcky než ty, které jsou uvedeny. Jsem si vědoma toho, že případné využití výsledků získaných v této práci mimo Univerzitu Karlovu je možné pouze po písemném souhlasu této univerzity.

Dále prohlašuji, že tato práce ani její podstatná část nebyla v žádné formě předložena k získání jiného nebo stejného akademického titulu na žádné vysoké škole nebo jiné instituci terciárního vzdělávání.

V Praze dne 26. 9. 2023 ……

Mgr. Sofiia Tvorynska

Experimental work included in this Ph.D. thesis was conducted in the period from 2018 to 2023 at the J. Heyrovský Institute of Physical Chemistry of the Czech Academy of Sciences, Department of Electrochemistry at the Nanoscale.

Acknowledgements

First and foremost, my most sincere appreciation goes to my supervisor Prof. RNDr. Jiří Barek, CSc. (Faculty of Sciences, Charles University) for his patience, excellent leading, dedicated support, and all opportunities offered to me at the beginning of my research career. Second, my huge thanks are expressed to supervisor-consultant Bohdan Josypčuk, Ph.D. (J. Heyrovský Institute of Physical Chemistry of the Czech Academy of Sciences) for the endless support, fruitful discussions, giving usable pieces of advice for my research, and readiness to assist in any possible way he was able throughout my Ph.D. studies. Furthermore, I would like to say my deep gratitude to Prof. Susana Campuzano for the kind guidance during my internship at Complutense University of Madrid and for expanding my knowledge on immunoassay, Dr. Maria Gamella for the invaluable help in the laboratory, and all my labmates for making my stay in Madrid an unbelievable experience. Additionally, my thanks belong to Dr. Olha Sarakhman (Slovak University of Technology in Bratislava) for her enthusiasm, everlasting moral support, and having always interesting discussions. I sincerely appreciate all other people involved in my research activities, especially from Department of Analytical chemistry (Faculty of Science, Charles University) and J. Heyrovský Institute of Physical Chemistry of the Czech Academy of Sciences.

I would like to thank to the organization "EURAXESS. CZ" for all the help related to the preparation and submission of documents for obtaining residence permits for me and my husband, which allowed me to be less distracted by these issues and focus on the research activity.

I am incredibly grateful to my husband Taras, brothers Mykola and Petro, sister Halyna, closest friends for their encouragement, and especially to my parents, Anna and Ihor, for their unwavering love and faith in me, without which I would not have been able to complete my studies.

Last, but not least, I express my boundless gratitude to the Armed Forces of Ukraine for the courageous protection of the sovereignty and independence of Ukraine and the safety of my family in particular. Only their invaluable work helped me not to lose heart during my Ph.D. studies.

Finally, I would like to acknowledge the following founding sources, which supported my research activities: the Specific University Research (SVV; projects no. 260440, 260560, and 260690), the Grant Agency of Charles University (project no. 1356120), and the Czech Science Foundation (projects no. 20-07350S and 20-01589S). My internship abroad was enabled due to the financial support provided by ERASMUS+ programme.

Contents

Abstract

This dissertation thesis presents the newly developed four highly reusable, stable as well as simple, and cost-effective electrochemical (bi)enzymatic biosensors for the selective and reliable determination of choline, acetylcholine, uric acid, and *L*-lactic acid in flow injection analysis. All biosensors are based on the concept of the spatial separation of the biorecognition part from detection one and amperometric monitoring of the enzymatically consumed oxygen *via* its four-electron reduction at the highly negative detection potential. In this way, the design of the biosensors includes an easily replaceable enzymatic mini-reactor(s) connected upstream to the flow cell that contains the appropriate silver amalgam-based transducer. The enzymatic mini-reactor based on choline oxidase, uricase, or lactate oxidase was used for choline, uric acid, or *L*-lactic acid biosensors, respectively. The acetylcholine bienzymatic biosensor includes the consequently connected choline oxidase- and acetylcholinesterase-based mini-reactors.

The first part of this thesis focuses on the construction of two different silver amalgam-based electrodes. Specifically, this section discusses the fabrication of a silver solid amalgam electrode covered by mercury film operating in a wall-jet cell and also highlights the differences between its utilization as a biosensor transducer and a tubular detector of polished silver solid amalgam integrated into the flow-through cell from an analytical and technical perspective. Besides, valuable solutions in the construction of the wall-jet cell are described. The second amalgam-based detector designed within this thesis is the first screen-printed silver amalgam electrode. This section presents valuable insights into the preparation strategy of these electrodes, their electrochemical characterization, and practical application, showcasing their potential in (bio)electroanalysis.

Special attention was dedicated to the selection of enzyme immobilization technique. Therefore, the second part of this thesis delves into a comparison of different covalent coupling protocols that differ in the type of crosslinking agent, the kind of support, its surface functional groups, and approaches to their synthesis, using glucose oxidase and laccase as test enzymes. This section provides useful insights into the elucidation of the relationship between the immobilization technique and the resulting biosensor performance, demonstrating that each component of the covalent attachment protocol has a noticeable impact. On the basis of this investigation, the most favourable immobilization protocol, namely the enzyme attachment through glutaraldehyde to mesoporous silica powder, MCM−41 or SBA−15, previously modified with (3-aminopropyl)triethoxysilane, was found. This protocol was used for the preparation of all enzymatic mini-reactors, the high enzymatic loading of which has been confirmed by determining the amount of immobilized enzyme using the Bradford method.

The following sections are devoted to the investigation of optimal biosensor operating conditions (pH and composition of the carrier solution, detection potential, flow rate, analyte injection volume, and time required for complete enzyme recovery), as well as the evaluation of analytical performance and selectivity of the biosensors. The results on the operational and storage stability indicate that the developed biosensors can be used for hundreds of measurements and stored for at least a year. The practical applicability of all elaborated biosensors was successfully confirmed by their use for the analysis of the relevant analyte-containing samples with varying degrees of matrix complexity (pharmaceuticals, food products, and human biological samples –urine and saliva).

Abstrakt

Předpokládaná disertační práce pojednává o čtyřech nově vyvinutých, opakovaně použitelných, stabilních a zároveň jednoduchých a cenově výhodných elektrochemických (bi)enzymatických biosenzorech pro selektivní a spolehlivé stanovení cholinu, acetylcholinu, močové kyseliny a *L*-mléčné kyseliny. Všechny biosenzory jsou založeny na koncepci prostorového oddělení biorozpoznávací části od detekční a amperometrického monitorování enzymaticky spotřebovaného kyslíku prostřednictvím jeho čtyřelektronové redukce při vysoce záporném detekčním potenciálu. Konstrukce biosenzorů zahrnuje snadno vyměnitelný enzymatický/é mini-reaktor(y) připojený/é před průtokovou celou, která obsahuje příslušný převodník na bázi pevného stříbrného amalgámu. Enzymatické mini-reaktory založené na cholin oxidase, urikase nebo laktát oxidase byly použity pro biosenzory na cholin, močovou kyselinu nebo *L*-mléčnou kyselinu. Bienzymatický biosenzor na acetylcholin zahrnuje sériově propojené mini-reaktory na bázi acetylcholinesterasy a cholin oxidasy.

První část této práce se zaměřuje na konstrukci dvou různých elektrod na bázi stříbrného amalgámu. Konkrétně tato část pojednává o výrobě stříbrné pevné amalgámové elektrody pokryté rtuťovým filmem pro wall-jet průtokovou celu a navíc, zdůrazňuje rozdíly mezi jejím využitím jako biosenzorového převodníku a tubulárního detektoru z leštěného stříbrného pevného amalgámu integrovaného do průtokové cely z analytického a technického hlediska. Kromě toho jsou popsána další řešení v konstrukci wall-jet cely. Druhým detektorem na bázi amalgámu a poprvé navrženým v rámci této práce je tištěná stříbrná amalgámová elektroda. Tato část poskytuje užitečné informace o přípravě těchto elektrod, jejich elektrochemické parametry a praktické aplikace, které ukazují na jejich možné využití v (bio)elektroanalýze.

Zvláštní pozornost byla věnována výběru techniky imobilizace enzymu. Proto se druhá část této práce zabývá porovnáním různých protokolů kovalentního spojování, které se liší typem síťovacího činidla, druhem podložky (nosiče), povrchovými funkčními skupinami a přístupy k jejich syntéze, přičemž jako testovací enzymy byly použity glukosa oxidasa a lakasa. Tato část poskytuje užitečné poznatky k objasnění vztahu mezi technikou imobilizace a výsledným výkonem biosenzoru a ukazuje, že každá složka protokolu kovalentního spojení má znatelný vliv. Na základě tohoto zkoumání byl nalezen nejvýhodnější imobilizační protokol, a to připojení enzymu prostřednictvím glutaraldehydu na mezoporézní práškový oxid křemičitý MCM−41 nebo SBA−15, předem modifikovaný (3-aminopropyl)triethoxysilanem. Tento protokol byl použit pro přípravu všech enzymatických mini-reaktorů, vysoký obsah enzymu v kterých byl potvrzen Bradfordovou metodou.

Následující části jsou věnovány zkoumání optimálních pracovních podmínek biosenzorů (pH a složení nosného roztoku, detekční potenciál, průtoková rychlost, objem vstřikovaného analytu a doba potřebná k úplnému obnovení aktivity enzymu), jakož i hodnocení analytického výkonu a selektivity těchto biosenzorů. Výsledky týkající se provozní a skladovací stability ukazují, že vyvinuté biosenzory lze použít pro stovky měření a skladovat po dobu nejméně jednoho roku. Praktická použitelnost všech vypracovaných biosenzorů byla úspěšně potvrzena jejich použitím pro analýzu příslušných vzorků obsahujících analyt s různým stupněm složitosti matrice (léčiva, potraviny a lidské biologické vzorky − moč a sliny).

Keywords

Acetylcholine
Acetylcholinesterase
Amalgam electrodes
Amperometric biosensor
Choline
Choline oxidase
Covalent immobilization
Enzymatic mini-reactor
Flow injection analysis
Four-electron oxygen reduction
Glutaraldehyde
Lactate oxidase
Lactic acid
Mesoporous silica powder
Oxygen consumption
Transducer based on silver amalgam
Uricase
Uric acid

Klíčová slova

Acetylcholin

Acetylcholinesterasa

Amalgámové elektrody

Amperometrický biosenzor

Čtyř-elektronová redukce kyslíku

Enzymatický mini-reaktor

Glutaraldehyd

Cholin

Cholin oxidasa

Kovalentní imobilizace

Mléčná kyselina

Močová kyselina

Laktát oxidasa

Mezoporézní prášek oxidu křemičitého

Průtoková vstřikovací analýza

Převodník na bázi stříbrného amalgámu

Spotřeba kyslíku

Urikasa

List of abbreviations and symbols

ACh	acetylcholine
AChE	acetylcholinesterase
AE	auxiliary electrode
A_{eff}	effective electrode surface area
AgA	silver amalgam
$AgA_{1.6}$-SPE	screen-printed silver amalgam electrode with diameter of working disc 1.6 mm
AgA_4-SPE	screen-printed silver amalgam electrode with diameter of working disc 4 mm
A_{geom}	geometric electrode surface area
$Ag_{1.6}$-SPE	screen-printed silver electrode with diameter of working disc 1.6 mm
Ag_4-SPE	screen-printed silver electrode with diameter of working disc 4 mm
AEAPTMS	[3-(2-aminoethylamino)propyl]trimethoxysilane
AEAEAPTMS	3-[2-(2-aminoethylamino)ethylamino]-propyltrimethoxysilane
APTES	(3-aminopropyl)triethoxysilane
BB	borate buffer
c	concentration
CB	carbonate buffer
Ch	choline
ChOx	choline oxidase
CEST	carboxyethylsilanetriol
CPG	aminopropyl-modified controlled pore glass
CS	carrier solution
DSS	disuccinimidyl suberate
EDC	*N*-(3-dimethylaminopropyl)-*N*′-ethylcarbodiimide
E_{det}	detection potential
Es	esterase from porcine liver
FIA	flow injection analysis
GA	glutaraldehyde
GC	glassy carbon
GOPTES	(3-glycidyloxypropyl)trimethoxysilane
GOx	glucose oxidase

Gr	graphite
ID	inner diameter
K_M^{app}	apparent Michaelis-Menten constant
LA	*L*-lactic acid
Lac	laccase
LDR	linear dynamic range
LOD	limit of detection
LOQ	limit of quantification
LOx	lactate oxidase
MF-AgSAE	silver solid amalgam electrode covered by mercury film
MSP	mesoporous silica powder
n	number of measurements
Na_2EDTA	disodium ethylenediaminetetraacete
NHS	*N*-hydroxy-succinimide
OD	outer diameter
PB	phosphate buffer
PHE	potential of hydrogen evolution
RE	reference electrode
RSD	relative standard deviation
SCE-AgA	saturated calomel electrode based on silver paste amalgam
SD	standard deviation
TD-p-AgSA	tubular detector of polished silver solid amalgam
TRIS	tris(hydroxymethyl)aminomethane
UA	uric acid
UOx	uricase
UOx(*B*)	Uricase from *Bacillus fastidiosus*
UOx(*C*)	Uricase from *Candida species*
v_{flow}	flow rate
V_{nj}	volume of the injected analyte
WE	working electrode

1 Aims of the work

This thesis has two main objectives. The first and foremost goal is to devise an electrochemical biosensing platform with the concept of using an enzymatic mini-reactor and monitoring oxygen consumption utilizing a silver amalgam-based transducer, which can be further used to achieve the second goal of developing reusable, simple and inexpensive amperometric biosensors for the selective and reliable determination of choline, acetylcholine, uric acid, and *L*-lactic acid in flow injection analysis.

The aims of this work were accomplished through the following steps:

(i) Construction of the two silver amalgam-based electrodes, specifically mercury film covered silver solid amalgam electrode constructed for a flow analysis and screen-printed silver amalgam electrodes.

(ii) Design of the flow cell adjusted in the wall-jet arrangement that provides a secure and effortless fixation of the working electrode to the inlet capillary.

(iii) Comparison of the different covalent techniques and support types to evaluate their impact on the biosensor performance.

(iv) Selection of the most favourable enzyme attachment protocol and preparation of the enzymatic mini-reactors.

(v) Optimization of the key operation parameters of the developed biosensors to achieve the best conditions for the determination of target analytes.

(vi) Assessment of the biosensor analytical characteristics, selectivity, repeatability, storage stability, and operation stability.

(vii) Verification of the practical applicability of the newly elaborated biosensors by their utilization for the analysis of the real samples.

The outputs received within the scope of this Ph. D thesis were reported in the following six scientific publications, available as Appendices 6.1 − 6.6 (Publication I − VI):

1. **S. Tvorynska**, J. Barek, B. Josypčuk, Amperometric biosensor based on enzymatic reactor for choline determination in flow systems, Electroanalysis, 31 (2019) 1901−1912.

2. **S. Tvorynska**, J. Barek, B. Josypčuk, Acetylcholinesterase-choline oxidase-based mini-reactors coupled with silver solid amalgam electrode for amperometric detection of acetylcholine in flow injection analysis, J. Electroanal. Chem., 860 (2020) 113883.
3. **S.Tvorynska**, J. Barek, B. Josypčuk, Flow amperometric uric acid biosensors based on different enzymatic mini-reactors: a comparative study of uricase immobilization, Sens. Actuators B Chem., 344 (2021) 130252.
4. B. Josypčuk, J. Langmaier, **S. Tvorynska**, Screen-printed amalgam electrodes, Sens. Actuators B Chem., 347 (2021) 130583.
5. **S. Tvorynska**, J. Barek, B. Josypčuk, Influence of different covalent immobilization protocols on electroanalytical performance of laccase-based biosensors, Bioelectrochemistry, 148 (2022) 108223.
6. **S. Tvorynska**, J. Barek, B. Josypcuk, High-performance amperometric biosensor for flow injection analysis consisting of a replaceable lactate-oxidase-based mini-reactor and a silver amalgam screen-printed electrode, Electrochim. Acta, 445 (2023) 142033.

2 Introduction

2.1 Amperometric enzyme-based biosensors: challenges associated with their application

Since C. Clark Jr. and Lyons introduced the first biosensor in 1962 [1], the demand for such analytical devices has been growing steadily. The main advantage of biosensors is a high degree of selectivity for the identification of the target analyte(s) due to the presence of a biorecognition element. Biosensors are classified according to the type of transducer and the type of biorecognition element. Depending on the transducer type, the biosensors divide into electrochemical (amperometric, potentiometric, conductometric or impedimetric), optical (colorimetric, fluorescent, luminescent), piezoelectric (acoustic, ultrasonic), and thermal. As biorecognition elements, enzymes, proteins, nucleic acids, antigens/antibodies, microorganisms, whole cells, and plant or animal tissues are utilized.

Among the various biosensors, amperometric enzyme-based ones are a class of the most numerous, proposed for a wide range of analyses, and successfully commercialized devices [2-4]. The major fields of their practical application are clinical diagnostics [5, 6], food industry [7, 8], pharmaceutical analysis [9], and environmental protection [10, 11]. The traditional amperometric enzyme-based biosensor has a pen-type configuration, *i.e.*, it represents an enzyme, immobilized on the surface of the working electrode (WE) (the so-called enzymatic electrode). Oxidases are the main class of enzymes used to prepare amperometric biosensors. Dehydrogenases are the second most common class of enzymes for this purpose. Unlike oxidases, they require an external cofactor, β-nicotinamide adenine dinucleotide, which should be located next to the enzyme, *i.e.,* immobilized on the WE surface, which leads to an additional immobilization step and complicates the biosensor design. Besides, the detection reaction based on the oxidation of the reduced form of β-nicotinamide adenine dinucleotide occurs with the formation of intermediates that cause the WE passivation [12].

During the oxidation of the substrate, the oxidase is reduced to its inactive form (Equation 1). In the presence of oxygen, the reduced form of the enzyme is oxidized back and hydrogen peroxide (H_2O_2) is formed (Equation 2).

$$\text{substrate} + \text{oxidase}_{\text{FAD}} \rightarrow \text{oxidase}_{\text{FADH}_2} + \text{product} \quad (1)$$

$$\text{oxidase}_{\text{FADH}_2} + O_2 \rightarrow \text{oxidase}_{\text{FAD}} + H_2O_2 \quad (2)$$

The detection can be based either on the oxygen reduction at the negative potential (Equation 3) or H_2O_2 oxidation at the positive one (Equation 4) (biosensor of the first generation).

$$O_2 + 2H_2O + 4e^- \rightarrow 4OH^- \quad (3)$$

$$H_2O_2 \rightarrow O_2 + 2H^+ + 2e^- \quad (4)$$

The latter principle is more commonly used, which can be explained by the large number of electrodes available that operate at positive potentials (platinum, gold, and glassy carbon electrode are the most popular ones). However, the high positive detection potential creates undesirable preconditions for the oxidation of a number of electrically active substances, such as ascorbic acid (AA), uric acid (UA), dopamine, acetaminophen, *etc.*, which leads to interferences [13, 14]. It is therefore essential to apply an electrode potential as low as possible.

One way to reduce the potential is to use a mediator (biosensor of the second generation). In general, a mediator is a low molecular weight particle that transfers electrons between the redox centre of an enzyme and the WE. During a catalytic reaction, the mediator first reacts with the reduced enzyme and then diffuses to the electrode surface to undergo rapid electron transfer. In order to function effectively, the mediator must react rapidly with the reduced enzyme, be nontoxic, and chemically stable (in both reduced and oxidized forms), and have a low redox potential. A detailed review dealing with the criteria that should be satisfied by a mediator can be found in [15]. The most common and well-known mediators are ferricyanide, ferrocene, and Prussian blue [12]. In addition, the mediator in tandem with the enzyme horseradish peroxidase (HRP) is widely used because it allows for operation at more negative potentials and, moreover, has a positive effect on the sensitivity of the biosensor [16]. However, the utilization of the mediators has some drawbacks. First of all, they may facilitate charge transfer between possible interferents and the electrode, increasing the interference problem. Second, the mediator and HRP should be immobilized on the WE surface, which significantly complicates the technology of the biosensor preparation (their leaching is a common problem). Besides, using additional enzyme HPR significantly increases the biosensor cost.

Another approach to avoid interference is to apply protective membranes to the surface of the WE above or below the enzyme layer, for example, by electropolymerization. The polymers that are used in such protective layers include phenylenediamine, polyeugenol, polypyrrole, as well as Nafion® and methylcellulose [17, 18]. In addition to protecting against the diffusion of interferents, these membranes often prevent the washing out of immobilized

enzymes and mediators, along with contamination of the sensitive surface by biomaterials (proteins, cell fragments) that are present in the sample (biofouling and electrode passivation are other issues related to the amperometric biosensor application for analysis).

An alternative approach that avoids the interference effect is to measure oxygen reduction. However, it requires an electrode that operates in the negative potentials. Until now, Clark-type electrode has been mainly used for this purpose [1]. One of the main disadvantages associated with its use is the difficulty of miniaturizing it to fit its design, which can cause inconvenience, especially when embedded in a flow-through cell. Oxygen detection is used much less frequently compared to indirect oxidation of H_2O_2, which may be due to the limited number of electrodes available for operation at highly negative detection potentials.

The major problem related to the application of the amperometric biosensors in analysis still remains their low storage stability and, more importantly, low operational stability (*i.e.*, reusability) [19]. One of the ways to solve this issue is the immobilization of the higher enzyme amount. In the case of enzymatic electrodes, the enzyme loading is limited by the surface area of the electrode. Therefore, only a small amount of the enzyme can be immobilized, which leads to its rapid depletion and, in turn, to short biosensor shelflife. The situation is even more complicated for the multienzymatic cascade biosensors, where two or three enzymes need to be immobilized (in addition, as mentioned in the previous paragraph, the mediator and HRP must also be attached to the WE surface in the case of H_2O_2 detection). Basically, the enzymatic electrodes are available only for tens of measurements/several hours of continuous work and lose their signal after several weeks of storage (see reviews [20-23]). It should be noted that in the vast majority of works available in the literature, the conclusion on the development of a highly functional biosensor can be questioned since it is based only on storage stability data, while operational stability has not been investigated.

2.1.1 Features of the amperometric enzyme-based biosensors in flow injection analysis

As compared with amperometric enzyme-based biosensors operated in batch-type mode, the biosensors in flow injection analysis (FIA) have the following advantages: (i) possibility of automation, (ii) high sample throughput, (iii) opportunity to vary the concentration detection range and sensitivity by changing the analyte injection volume (V_{inj}) and flow rate (v_{flow}), and (iv) lower consumption of the substrate and supporting electrolyte. In addition, the problem of

WE passivation in FIA is less noticeable than in the batch-mode, since the WE is in contact with the sample zone for a very short period of time.

Besides, in FIA, there is an exceptional possibility to construct a biosensor with spatially separated biorecognition and detection parts. Accordingly, this means that the enzyme instead of on the WE surface is attached to a specific support, forming an enzymatic mini-bioreactor that is located upstream of the flow cell containing the transducer. The major advantage of this approach, in contrast to the enzyme electrodes, relies on the opportunity to immobilize the notably higher enzyme amount, which leads to the improvement of biosensor lifetime and reusability [24-26]. In addition, enzymatic mini-reactors are easily replaceable, which means that changing the type of biosensor from detecting one analyte to another is quickly done by simply changing the mini-reactor (the rule works: one transducer − many biosensors).

There are different arrangements of mini-reactors such as membrane [27], wall-coated capillary [28], monolith-based [29], and packed-bed [30]. The latter, which involves immobilizing the enzyme on solid support characterized by a large surface area (porous powder or beads) and then packing them in any tube, is the most common, as it is the simplest one and allows for the highest enzyme load. Among different enzyme immobilization methods, covalent coupling with glutaraldehyde (GA) is the most widespread. Regarding support type, beads, including magnetic, oxirane acrylic, porous chitosan, and aminopropyl-modified controlled pore glass (CPG) are utilized. Among the powdered supports, the mesoporous silica powders (MSPs) are the prospective candidates due to a large surface area, high enzyme loading capacity, biocompatibility, inertness, and a possibility to be easily modified by the different functional groups *via* silanization technique [31-35].

The biosensors based on enzyme mini-reactors have been proposed for a large scale of analytes (cholesterol [28], glutamate [36], glucose [37, 38], phenolic compounds [39, 40], AA [41, 42], H_2O_2 [43], putrescine [44], pesticides [45], lactose [46] *etc.*), demonstrating the good results on the operational stability. For instance, Azevedo *et al.* constructed the ethanol biosensor with the mini-reactors based on the covalent immobilization of alcohol oxidase *via* GA on CPG. It was reported that the biosensor showed 95% of its initial signal after the 33 600 injections of the 25 μL of 6.5 mM ethanol [47]. Prodomidis *et al.* proposed the mini-reactor containing the glycerol dehydrogenase, which retained 85% of its activity after 2500 injections over 3 months [30].

The configuration of spatially separated enzyme parts has been successfully used to construct multienzymatic cascade biosensors [48-53]. In this case, biosensors can consist of a single mini-reactor [48, 52, 53], where all enzymes are placed, or a set of separate

reactors [49-51]. An overview of some previously proposed biosensors based on multienzymatic cascade mini-reactors that have shown high reusability is given in **Table 2.1**.

Table 2.1. The biosensors based on multienzymatic cascade mini-reactors with high operational stability.

Analyte	Enzymatic mini-reactor(s)		Operational stability	Ref.
	Enzymes	Support/ Immobilization method		
Octopine	#1Octopine dehydrogenase #2 Pyruvate oxidase	Chitosan beads/ covalent *via* GA	50 assays/30 days	[48]
Ornithine	#1 Ornithine carbamyl transferase #2 Pyruvate oxidase	CPG/ covalent *via* GA	150 assays/30 days	[49]
Fish freshness	#1 Alkaline phosphatase #2 Nucleoside phosphorylase #3 Xanthine oxidase	CPG/ covalent *via* GA	700 assays/60 days	[50]
Fish freshness	#1 Inosine-5'-monophospate #2 Nucleoside phosphorylase #3 Xanthine oxidase	Chitosan beads/ covalent *via* GA	200 assays/30 days	[51]

It should be noted that the operational stability of biosensors strongly depends on the concentration they detect (the higher the concentration, the lower the operational stability).

2.2 Silver amalgam electrodes in (bio)electroanalysis

Solid amalgam has become widely used electrode material after Novotny and Yosypchuk introduced it in 2000 as an alternative to mercury [54]. Among the various amalgam electrodes, differing in the amalgam form (solid, paste, composite) and metal for its preparation (Ag, Au, Bi, Cu, *etc.*), the use of silver solid amalgam electrodes (AgSAEs) as detectors in electrochemical analysis has achieved unprecedented popularity [55-57].

The AgSAEs not only provide the same desirable electrochemical properties as mercury electrodes, including a high hydrogen overvoltage and a wide range of working potentials, but at the same time offer some benefits not inherent to them. First of all, they are mechanically stable, which makes them suitable for electroanalysis with a flow-through arrangement (FIA, HPLC). The other distinct advantages are the simple, reproducible, and low-cost design procedure, convenient handling, easy and quick regeneration of an electrode's surface in the case of its passivation, and the possibility to construct them in any size or shape. Moreover, due to the formation of strong covalent thiol bonds (Hg−S−), the surface of the AgSAEs can be further modified [58, 59]. Lastly, it is worth emphasizing that amalgam electrodes are non-toxic and compatible with the concept of "green analytical chemistry". The surface of AgSAE was proved to form the crystalline structure Ag_2Hg_3, and no other phases, liquid mercury, or pores were observed [55]. Furthermore, measuring the possible mercury vapour pressure from the AgSAEs using atomic absorbtion spectroscopy verified that mercury does not evaporate from the solid amalgam, confirming that these electrodes are environmentally friendly [60].

The preparation of AgSAE basically relies on the amalgamation of the fine silver powder (particle size 5 − 10 μm) and lasts a couple of hours. The electrode prepared in this way is called polished AgSAE (p-AgSAE) as its surface might be pre-treated by polishing with Al_2O_3 suspension. Since solid amalgam is well wetted by mercury, p-AgSAE can be easily covered by mercury meniscus (m-AgSAE) or mercury film (MF-AgSAE) by the electrochemical deposition or just by p-AgSAE immersing into the liquid mercury for several seconds [55].

A large number of the voltammetric/amperometric methods using p-AgSAE/MF-AgSAE/m-AgSAE in a batch arrangement was developed for the sensitive, reliable, and rapid determination of the various reducible inorganic and organic compounds (*e.g.*, pesticides [61], pharmaceuticals [62, 63], vitamins [62, 64], food additives [65], *etc.*). Amalgam electrodes have also been successfully used for the voltammetric analysis of synthetic oligonucleotides, purine bases, and acid-treated DNA together with DNA damage detection and hybridization of DNA [66-69]. It is worth emphasizing that due to the possibility of measurement at highly negative

potentials (up to −2 V in aqueous solutions), the AgSAEs allow to study substances and processes, which are mostly unavailable with other existing solid electrodes.

The introduction of mechanically stable AgSAEs has significantly contributed to the development of electrochemical detecting methods in flow-through systems. For instance, the p-AgASE adjusted in a wall-jet and thin-layer arrangements was applied for the amperometric determination of a mixture of plant grow stimulators nitrophenols using HPLC [70]. Further, the methods for the determination of the environmental pollutants (*e.g.,* 5-nitroquinoline [71] and nitro derivatives of polycyclic aromatic hydrocarbons [72]) and N-nitroso antineoplastic drug carmustine [73] were elaborated employing the combination of HPLC/FIA with amperometric detection at m-AgSAE incorporated in the wall-jet arrangement. The tubular detector based on silver solid amalgam (TD-p-AgSA) in flow-through cell, constructed within the framework of O. Josypčuk's Ph. D. thesis [74], was successfully used for the determination of the lomustine in pharmaceutical preparation by non-stop-flow differential pulse voltammetry [75].

In addition to electrochemical sensing, another very promising area in which AgSAEs can be particularly useful is biosensing. Due to the aforementioned advantages, AgSAEs can be a good alternative to Clark electrodes for monitoring O_2 consumption in the development of amperometric biosensors. The oxygen reduction on the mercury covered AgSAEs occurs *via* two two-electron consecutive steps similar to pure mercury electrodes [76]:

(i) $O_2 + 2H^+ + 2e^- \rightarrow H_2O_2$ (acid solution) or
$O_2 + 2H_2O + 2e^- \rightarrow H_2O_2 + 2OH^-$ (neutral or alkaline solution) (~ −0.1 V *vs*. SCE)

(ii) $H_2O_2 + 2H^+ + 2e^- \rightarrow 2H_2O$ (acid solution) or
$H_2O_2 + 2e^- \rightarrow 2OH^-$ (alkaline solution) (~ −0.9 V *vs*. SCE)

The high negative potential of hydrogen evolution (PHE) on AgSAE enables its application for oxygen reduction *via* overall four-electron transfer.

The first biosensor consisting of the AgA-based transducer was proposed within the framework of O. Josypcuk's Ph.D. thesis [74]. Specifically, a glucose biosensor based on the detection of oxygen consumption employing the TD-p-AgSA was successfully developed [77].

2.3 Analytes of interest: choline, acetylcholine, uric acid, and *L*-lactic acid

2.3.1 Functions and importance of the detection

Choline (Ch, IUPAC name: 2-hydroxy-*N*,*N*,*N*-trimethylethan-1-aminium) is an essential water-soluble micronutrient with an amino acid-like structure. Although it is not formally classified as a vitamin, it is often referred to as a B complex vitamin due to its similarities and is called vitamin B_4. Ch affects a number of vital body functions. First, it is the precursor for the production of acetylcholine, the importance of which is described below. Second, Ch is the main source of methyl groups *via* its metabolite, betaine, and it is important in the synthesis of two essential phospholipids, phosphatidylcholine and sphingomyelin, that provide structure to cell membranes and facilitate transmembrane signalling. Additionally, like folate, Ch also plays a critical role during fetal development, affecting neural tube development, as well as stem cell proliferation and apoptosis, which affect brain structure and function throughout life [78].

In healthy adults, the concentration of Ch in plasma ranges from 9.5 to 13.3 μmol L^{-1} (14.5 – 17.1 μmol L^{-1} during pregnancy [79]). Changes in serum Ch levels are associated with a variety of human diseases. Ch deficiency leads to acetylcholine (ACh) deficiency, which in turn can result in neurodegenerative disorders related to impaired attention, memory, and cognitive abilities (see the paragraph on ACh). Moreover, the prolonged decreased Ch content manifests in various liver diseases, cardiovascular disorders, and muscle damage [80]. Finally, the abnormal low Ch concentration causes an elevated homocysteine level, which increases the risk of complications during pregnancy, premature birth, and very low childbirth weight [78]. On the other hand, the elevated Ch level is associated with oncogenesis and tumour progression [81]. It was found for almost every cancer type that cancer cells affect the activity of several Ch transporters as well as of enzymes, Ch kinase-α, phospholipase *C* and *–D*, and glycerophosphocholine phosphodiesterases), which lead to a rise in phosphocholine and total Ch level. It has been reported that men with the abnormal high Ch had a 70% increased risk of lethal prostate cancer [82].

Some amount of Ch is synthesized *de novo* in the liver, mostly as phosphatidylcholine, however, it is not sufficient to meet human needs. Therefore, to ensure healthy body functionality, most of the Ch should come from the diet. Ch is present in a variety of foods as

free Ch, but is also present in esterified forms such as phosphocholine, phosphatidylcholine, glycerophosphocholine, and sphingomyelin. Foods that contain high levels of Ch include beef liver (414 mg/100 g), which is one of the richest sources, egg yolks (the yolk of one large egg contains almost 140 mg), meat, fish, dairy products, whole grains, soybeans, and broccoli. In addition, to avoid shortages, Ch chloride and bitartrate are commercially available in the form of dietary supplements and sports nutrition. The current adequate daily intake of Ch ranges from 125 mg/day in infants up to 6 months of age to 550 mg/day in adult men and breastfeeding women [79]. For infants, where nutritional intake is limited to a single source, Ch supplementation can be extremely important. For breast-fed infants, Ch is transported from the mother's blood to the milk to promote growth and brain development. To match this intake in formula-fed babies, Ch is a mandatory additive in many infant formulas.

Therefore, the assessment of Ch concentration in biological fluids for clinical analysis, as well as in medicines, dietary supplements, and infant formulas for quality control during their manufacture is in great demand.

Acetylcholine (ACh, IUPAC name: 2-acetoxy-*N*,*N*,*N*-trimethylethanaminium) is an important neurotransmitter and neuromodulator, which is produced from Ch in the presence of acetyl-coenzyme-A and enzyme choline acetyltransferase, and released from the nerve cells to transfer signals to the other cell types. It plays a key role in both the peripheral and central nervous systems, as it is implicated in all muscle movements and mental processes such as attention, cognition, learning, and memory formation [83]. Accordingly, the decrease in ACh level (<10 μmol L^{-1}) leads to various neurological disorders, including Parkinson's disease [84], schizophrenia, dementia, and Alzheimer's disease [85]. The latter ranks fourth in the causes of death among adults [86]. Therefore, the identification of ACh deficiency is key factor in terms of early diagnosis of the abovementioned disorders and their treatment. On the other hand, excessive accumulation of ACh causes symptoms of both muscarinic and nicotinic toxicity, including cramps, muscle fasciculation (twitching) and weakness, paralysis, diarrhoea, increased salivation, lacrimation, and blurry vision [87]. For all these reasons, knowledge of ACh levels is crucial in the decision-making process in clinical practice.

Uric acid (UA, IUPAC name: 2,4,6-trihydroxypurine) is the final product of the purine metabolism pathway in the human body, which is excreted mainly by the kidneys and intestinal tract. The blood serum concentration of UA is determined by the balance of its formation and excretion. Any deviations from the normal range (1.49 – 4.46 mmol L^{-1} in urine and 0.13 – 0.46 mmol L^{-1} in human blood serum [88]) indicate a wide range of pathological states.

For example, the excess of UA (hyperuricemia) leads to the accumulation of urate crystals, usually in the joints of the extremities and kidneys, causing gout (inflammation, swelling, and redness of a joint, such as a toe or knee, accompanied by intense pain) and the various kidney diseases [89]. In addition, an abnormal high level of UA in blood serum is linked with diabetes [90], cardiovascular diseases [91], and is an indicator of the Lesch-Nyhan syndrome, a rare X-linked recessive genetic disorder characterized by the lack or deficiency of the enzyme hypoxanthine-guanine phosphoribosyltransferase, which is involved in the purine metabolism (most often affects males [92]). On the other hand, abnormally low UA content is a symptom of multiple sclerosis [93]. Hence, estimation of the UA concentration in urine and blood serum is a valuable diagnostic marker.

***L*-lactic acid** (LA, IUPAC name: 2-hydroxypropanoic acid) is a key metabolite in the process of anaerobic glycolysis in muscles, erythrocytes, and brain. Generally, the range of LA in serum for healthy people is 0.5 – 2.2 mmol L^{-1} at rest and increases up to 12 mmol L^{-1} during exercise. During intense physical activity when muscles are pushed over the aerobic threshold, the oxygen uptake rate significantly limits the amount of available oxygen leading to intensive LA generation, where its content can reach 25 mmol L^{-1} [12]. In the normal state, the LA level decreases at the approximate rate of 320 mmol L^{-1} h^{-1}, returning to the normal values in 5 min, due to the liver and kidney metabolism along with the re-conversion to the pyruvic acid by the enzyme lactate dehydrogenase [17].

However, the accumulation of LA (lactic acidosis), caused by its constant hyperproduction (*reason i*) or pathology of its cleavage (*reason ii*), is an indicator of a number of diseases and pathological conditions. First of all, the elevated LA resulted from *reason i* is linked with ischemic situations, which can be caused by all types of shock, hypoxia, sepsis, suffocation and respiratory insufficiency, and carbon monoxide or drug intoxication. Therefore, in the intensive care unit, the LA level is measured in the dynamics of assessing the severity of the patient's condition, predicting the probability of mortality, and evaluating of treatment effectiveness and control of its adequacy [94, 95]. For instance, hyperlactatemia (>5 mmol L^{-1}) in combination with severe acidosis (blood pH<7.35) gives a prediction of 80% mortality [95]. Besides, the increased LA concentration caused by *reason ii* indicates diabetes or absorptive abnormalities of short-chain fatty acids in the colon [96]. Moreover, LA is a potential biomarker for cancer and metastases, the malignant transformation of normal cells into tumour ones was reported to be accompanied by the LA accumulation [97].

In addition to clinical analysis, the determination of LA is important for other fields. In sports as well as space medicine, monitoring of LA concentration during exercise is used with

the aim of training and evaluating performance endurance, the so-called lactate threshold [12], which indicates the physical training level in athletics/cosmonauts. The food industry monitors the LA contents to control the course of the fermentation processes in dairy products and estimate the freshness and quality of the food products in total [98]. In the winemaking industry, the increasing concentration of LA is monitored for assessment of the course of malolactic fermentation, which is based on the conversion of the tart-tasting malic acid, naturally present in grape must, into softer- and creamier-tasting LA, leading to a lowering of the overall acidity and tartness of the wine. The content of LA in wine usually amounts to up to 3 g L^{-1} [99].

2.3.2 Methods of determination

To date, various methods for the determination of Ch, ACh, UA, and LA have been described. As shown in the reviews [100-103], techniques, such as high-performance liquid chromatography and gas chromatography in combination with different detectors, electrochemical, flame ionization, or mass spectrometic, are some of the most frequently used for the analyses of all four above-mentioned analytes. Despite the extremely low limits of detection and good selectivity, complex and sophisticated equipment is an apparent limitation of these methods. Besides, the utilization of such techniques for the analysis of UA and LA may be regarded as somewhat unsubstantiated, as the levels of these analytes tend to lie in the tens to hundreds micromolar range in most samples.

Neither ACh nor Ch is electroactive. Instead, due to the presence of the electroactive groups in UA and LA, the electrochemical methods for their analysis are also frequently applied. Accordingly, a variety of amperometric and voltammetric sensors for the quantification of UA and LA, which are based on their direct oxidation on different electrodes, bare and modified have been reported [104, 105]. Although the electrochemical sensors provide simple, rapid, and cost-effective determination, their application in routine practice is limited by poor selectivity, which is caused by the oxidation of both target analytes and other electrochemically oxidizable compounds (*e.g.*, AA, dopamine) at close potentials. Furthermore, the modified electrodes tend to be characterized by complex architectures along with low mechanical stability, while their preparation procedure is time-consuming and labour-intensive.

Amperometric enzyme-based biosensors for Ch, ACh, UA, and LA analysis can be an acceptable alternative to the aforementioned methods due to their high selectivity, good sensitivity, fast response, simplicity, portability, and convenient operation. Thus, the enzyme

choline oxidase (ChOx) is used for the preparation of the Ch biosensors, while the amperometric ACh biosensors are based on the cascade enzymatic reactions involving two enzymes, AChE and ChOx. The biosensors for the UA determination include the enzyme uricase (UOx). The LA biosensors can be based on either lactate dehydrogenase or lactate oxidase (LOx) − the latter is used more frequently.

Hundreds of biosensors are available in the literature for each of these four analytes. The principles of their construction and operation as well as the advantages and disadvantages can be found in special reviews [17, 21, 88, 106, 107]. Based on the above-mentioned reviews, it is easy to see that most of the proposed biosensors have a classical pen-type configuration, the detection principle of which is based on direct/indirect (using mediators and/or enzyme HRP) oxidation of H_2O_2, and they are used for analysis in a batch arrangement. It should be noted that in the vast majority of papers, results are given only regarding the storage stability and no data on biosensor operational stability are indicated. Available data show no biosensors with high operation stability. Such a conclusion was made, since the significant loss of the biosensor signals (>50%) were already observed after tens of measurements or several hours of the continuous use. Additionally, as reported in the review [17], only a half of the proposed LA biosensors was tested for the real samples.

Table 2.2 presents overview of the previously reported amperometric biosensors based on the enzymatic mini-reactors for the determination of Ch, ACh, UA, and LA (none of them is based on the O_2 monitoring). The constructed Ch biosensor demonstrates the high storage stability; however it is based on the direct H_2O_2 oxidation, which could present a major obstacle in biosensor application for the analysis of real samples [108]. To our knowledge, two amperometric biosensors based on the enzymatic mini-reactors were proposed for the determination of ACh [109, 110]. However, in these papers, only one enzyme of the AChE/ChOx bienzyme system was immobilized in the reactor, while the second one – on the surface of the WE. Moreover, in [110], the third enzyme catalyse was used. For the UA quantification, Wang *et al.* [111] proposed the biosensor comprising the UOx-mini-reactor in the combination with the porous carbon felt electrode modified with the mediator thionine and HRP. Although the preparation of both reactor and modified electrode was simple and fast (*e.g.*, 30 min for the reactor), the proposed biosensor exhibited very low storage stability. As shown in **Table 2.2**, among three biosensors proposed for the LA determination, two of them exhibit high operational stability [112, 113]. However, both are based on the direct oxidation of H_2O_2. Additionally, the LA biosensor proposed in [114] showed the low sensitivity. In contrast, the third LA biosensor demonstrated high sensitivity, but its design is more complex

than the previous two due to the additional immobilization of the mediator and HRP on the surface of the WE. Characteristics of all biosensors with general comments on their features are given in **Table 2.2**.

In summary, the design of biosensors that meet all the criteria, namely high operational stability, selectivity, simple and inexpensive configuration, and easy preparation procedure, for the reliable determination of Ch, ACh, UA, and LA is still of great demand.

Table 2.2 Overview of the previously proposed amperometric biosensors based on the enzymatic mini-reactors for the determination of Ch, ACh, UA, and LA in FIA.

Analyte (Ref.)	Enzymatic reactor(s)	Transducer	Detection	LOD / µmol L^{-1}	Stability	General comments
Ch ([108])	Covalent immobilization of ChOx *via* GA on CPG	Pt electrode covered with a polypyrrole membrane	H_2O_2, +0.7 V *vs.* Ag/AgCl	7	Storage: >1 year Operational: 70% over 2 months of regular use	▪ No interference study ▪ Determination in milk hydrolysates
ACh ([109])	Encapsulation of AChE inorganically modified sol-gel glass	Graphite paste electrode modified by ChOx and mediator tetrathiafulvalene	Mediator, +0.24 V *vs.* Ag/AgCl	Not reported	Storage (for the reactor): 100% over 4 months	▪ No data on the storage and operation stability for the whole biosensor
ACh ([110])	Covalent immobilization of ChOx and catalase *via* GA on magnetic Fe_3O_4 nanoparticles modified by (3-aminopropyl)triethoxysilane	Glassy carbon electrode modified by AChE, ChOx and mediator Prussian blue	Mediator, −0.05 V *vs.* Ag/AgCl	1	Operational (for reactor): at least 10 days (3 – 6 h of use each day) Operational (for transducer): at least 1 h of use	▪ Monitoring of ACh release in rat brain by integration biosensor and *in vivo* microdialysis
UA ([111])	Physical adsorption of UOx on porous carbon felt (enzyme was not washed out at least 3 h of its continuous use)	Porous carbon felt electrode modified by HRP and mediator thionine (prepared every time before measurement)	HRP intermediates, −0.05 V *vs.* Ag/AgCl	0.18	Storage: 63%/over 7 days	▪ Up to 90 samples/h ▪ Analysis of human plasma and urine
LA ([112])	Covalent immobilization of LOx *via* GA on CPG	Pt electrode coated with the m-phenylenediamine layer	H_2O_2, +0.6 V *vs.* Ag/AgCl	100	Operational: 1000 measurements	▪ 50 samples/h ▪ Analysis of blood serum and milk products ▪ Simultaneous glucose detection using glucose oxidase-based reactor
LA ([113])	Covalent immobilization of LOx *via* GA on protein membrane (pig small intestine)	Glassy carbon electrode	H_2O_2, +0.59 V *vs.* Pd electrode	50	Operational: signal decrease after 800 measurements	▪ 40 samples/h ▪ Analysis of dairy products ▪ Comparison of two LOx
LA ([114])	Covalent immobilization of LOx *via* GA on CPG	Glassy carbon electrode modified by HRP and Os-based mediator complex	Mediator, 0.0 V *vs.* Ag/AgCl	0.005	Operational: no decrease of biosensor signal after analysis of 20 milk samples	▪ 30 samples/h ▪ Analysis of milk dairy products ▪ Rotating reactor

3 Results and discussion

Almost all results presented in this thesis have been published in six papers in international peer-reviewed journals, which are available as Appendices ***Publication I****,* ***II****,* ***III****,* ***IV****,* ***V****, and* ***VI*** *in Chapter 6. In addition, they are referred to [****115-120****] (and highlighted in* ***bold****) in this Chapter.*

Within this thesis, four reliable, cost-effective, highly stable, and reusable electrochemical enzymatic biosensors for FIA have been successfully developed and constructed, in particular for the determination of Ch [**115**], ACh [**116**], UA [**117**], and LA [**120**]. Importantly, the fabricated ACh biosensor, contrary to three others, is a bienzymatic. The concept of all the proposed biosensors is based on two key features:

(i) spatial separation of biorecognition and detection parts;

(ii) use of the silver amalgam (AgA)-based transducer for monitoring of oxygen consumption.

A brief overview of the developed biosensors, including their construction (biorecognition and detection parts) and operating principle (simplified schematic representation of the enzymatic and electrochemical reactions) is given in **Table 3.1**.

Essentially, the biorecognition part is presented as an enzymatic mini-reactor consisting of $-NH_2$ functionalized MSP as support (either SBA15-NH_2 or MCM41-NH_2) covalently coated through GA with the appropriate enzyme and placed into a Plexiglas® tube (inner diameter (ID) 4 mm, outer diameter (OD) 6.4 mm, length 15 mm). Accordingly, the enzymatic mini-reactors based on ChOx (ChOx−SBA15-$NH_{2\,(GA)}$) [**115**], UOx (UOx−MCM41-$NH_{2\,(GA)}$) [**117**], and LOx (LOx−SBA15-$NH_{2\,(GA)}$) [**120**] were prepared, and used as the biorecognition part for the Ch, UA, and LA biosensors, respectively. The ACh biosensor includes the consequently connected mini-reactor based on AChE (AChE−SBA15-$NH_{2\,(GA)}$) with ChOx−SBA15-$NH_{2\,(GA)}$ one [**116**].

The detection part includes the measurement of the enzymatically consumed oxygen by its amperometric four-electron reduction at a highly negative detection potential on the AgA-based transducer. It is worth noting that three different types of AgA-based transducers with flow cells of different configurations were utilized, as follows: TD-p-AgSA, embedded in the flow-through cell, MF-AgSAE with the wall-jet cell, and screen-printed silver amalgam electrode (AgA-SPE) in the wall-jet cell for SPEs. Importantly, the latter two detectors, together

with the wall-jet cell of the improved design for MF-AgSAE, were developed and constructed as part of this thesis. The rationale for choosing the detector for each of the proposed biosensors is stated below in ***subchapter 3.1***.

Table 3.1 An overview of all developed biosensors.

Analyte	**Biosensor**	
(Ref.)	**Enzymatic mini-reactor(s)**	**Transducer**
Ch ([**115**])	ChOx−SBA15-NH_2 (GA)	MF-AgSAE
	Enzymatic reaction:	*Electrochemical reaction:*
	choline + H_2O + $2O_2$ $\xrightarrow{\text{ChOx}}$ betaine + $2H_2O_2$	$O_2 + 2H_2O + 4e^- \rightarrow 4OH^-$ (−1.4 V *vs.* SCE-AgA)
ACh ([**116**])	AChE−SBA15-NH_2 (GA) ChOx−SBA15-NH_2 (GA)	MF-AgSAE
	Cascade enzymatic reactions:	*Electrochemical reaction:*
	acetylcholine + H_2O $\xrightarrow{\text{AChE}}$ choline + acetic acid choline + H_2O + $2O_2$ $\xrightarrow{\text{ChOx}}$ betaine + $2H_2O_2$	$O_2 + 2H_2O + 4e^- \rightarrow 4OH^-$ (−1.4 V *vs.* SCE-AgA)
UA ([**117**])	UOx−MCM41-NH_2 (GA)	TD-p-AgSA
	Enzymatic reaction:	*Electrochemical reaction:*
	uric acid + H_2O + O_2 $\xrightarrow{\text{UOx}}$ allantoin + CO_2 + H_2O_2	$O_2 + 2H_2O + 4e^- \rightarrow 4OH^-$ (−1.1 V *vs.* SCE-AgA)
LA ([**120**])	LOx−SBA15-NH_2 (GA)	$AgA_{1.6}$-SPE
	Enzymatic reaction:	*Electrochemical reaction:*
	lactic acid + O_2 $\xrightarrow{\text{LOx}}$ pyruvic acid + H_2O_2	$O_2 + 2H_2O + 4e^- \rightarrow 4OH^-$ (−0.9 V *vs.* Ag pseudo-RE)

Abbreviations: $AgA_{1.6}$-SPE – silver amalgam screen-printed electrode (diameter of the working amalgam disc is 1.6 mm), Ag pseudo-RE – silver pseudo-reference electrode, SCE-AgA – saturated calomel electrode based on the silver amalgam.

Fig. 3.1(A-C) demonstrates photographs of the developed biosensors, each of which consists of the corresponding easily replaceable enzymatic mini-reactor (or two mini-reactors for the ACh biosensor) positioned in front of the appropriate flow cell containing the AgA-based transducer.

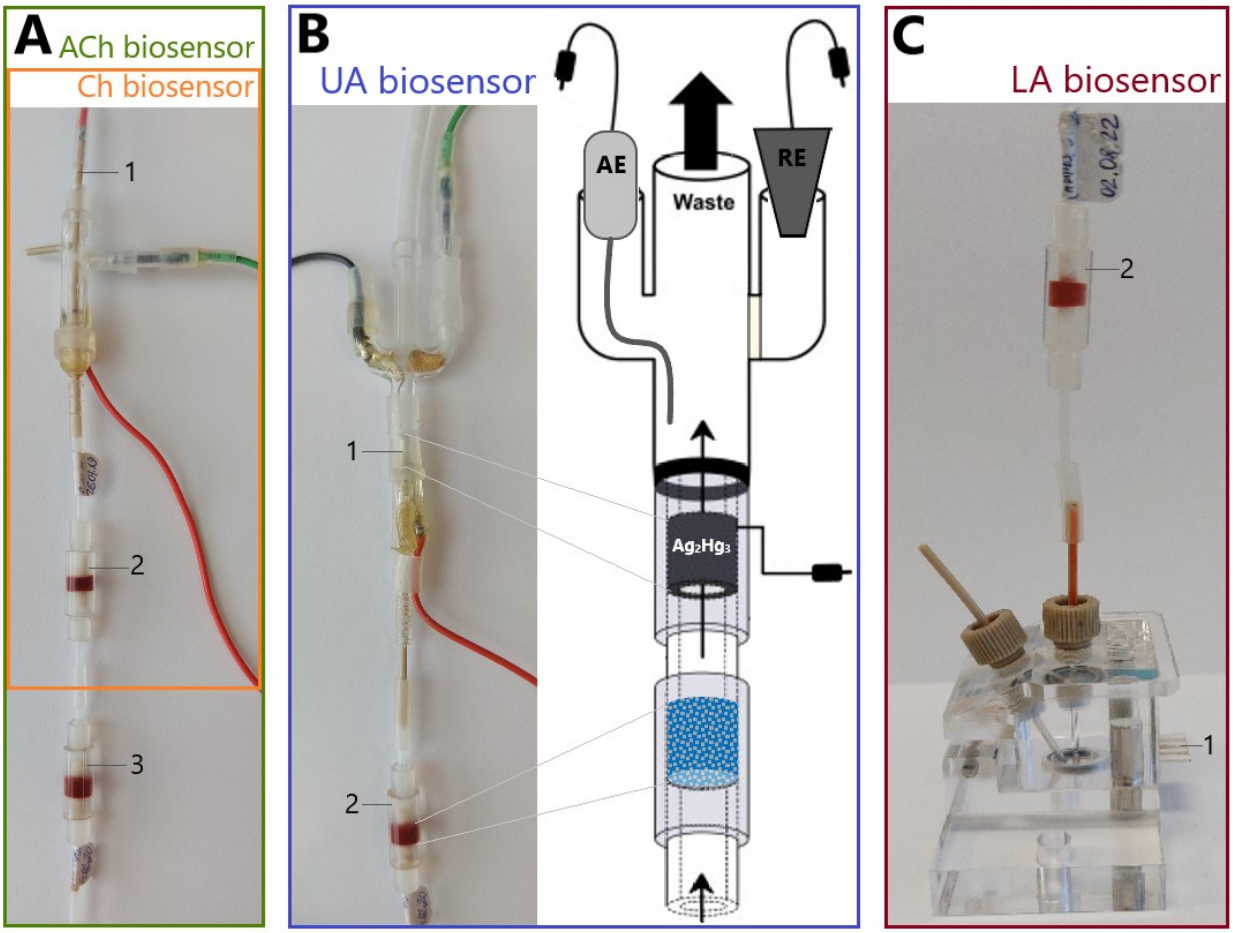

Fig. 3.1 (**A**) – Photograph of the developed ACh biosensor consisting of the MF-AgSAE (*1*) integrated in the wall-jet cell and two enzymatic mini-reactors, first with ChOx (*2*) and second with AChE (*3*). If the AChE-based mini-reactor (*3*) is disconnected, it is the Ch biosensor. (**B**) − Photograph and scheme of the elaborated UA biosensor consisting of the TD-p-AgSA (*1*) incorporated in the flow-through cell and the UOx-based mini-reactor (*2*). (**C**) – Photograph of the proposed LA biosensor containing the $AgA_{1.6}$-SPE (*1*) integrated in the wall-jet cell for SPEs and the LOx-based mini-reactor (*2*).

As shown in **Fig. 3.2**, the almost constant baseline current with a negative sign was recorded when the injection zone did not contain the target analyte (dashed lines).

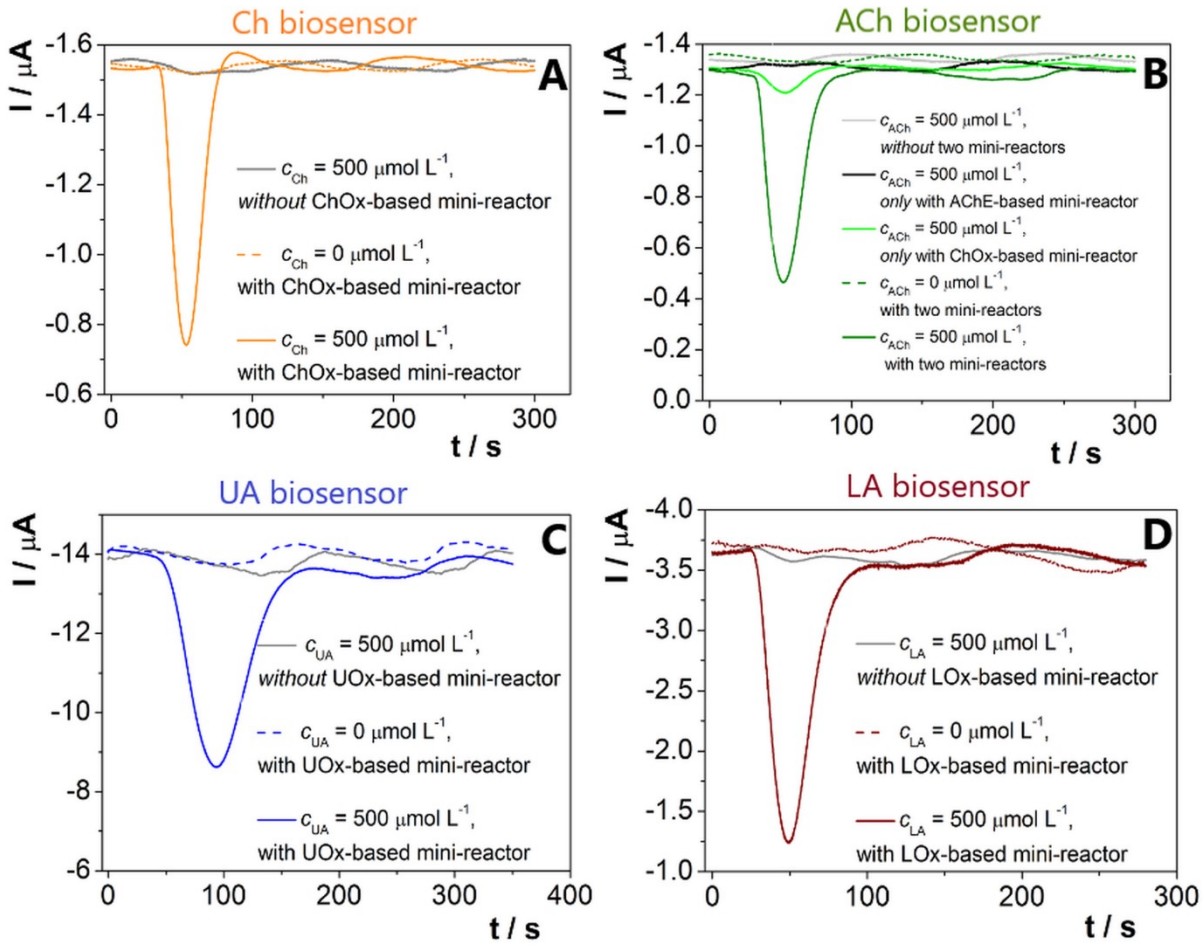

Fig. 3.2 Amperometric responses of Ch biosensor (**A**), ACh biosensor (**B**), UA biosensor (**C**), and LA biosensor (**D**) to 0 and 500 µmol L^{-1} of the corresponding analyte when the target enzymatic mini-reactor(s) are connected and disconnected.

However, when the analyte-containing injection zone (where, the analyte is either Ch, UA, or LA) passed through the respective mini-reactor, the analyte was oxidized by the immobilized enzyme. In the case of the ACh biosensor, ACh was first enzymatically hydrolysed in the AChE-based mini-reactor to form Ch, followed by further Ch oxidation in the second mini-reactor containing ChOx. As can be seen from the reactions presented in **Table 3.1**, the enzymatic conversion of Ch, UA, and LA, as well as the cascade enzymatic reactions for ACh, are accompanied by oxygen consumption. As a result, when the injection zone reached the AgA-based transducer, to which a potential for the amperometric measurement of four-electron oxygen reduction was applied, a downward peak was recorded due to the level of the dissolved oxygen in the injection zone being lower than in the rest of the carrier solution (CS). The decrease in the oxygen content is proportional to the analyte concentration.

For the purpose of proof of concept, the measurements were also conducted without the enzymatic mini-reactors. In the case of the Ch, UA, and LA biosensors, neither upward nor downward peaks were recorded, as depicted in **Fig. 3.2(A, C, D**; grey lines), while the ChOx-, UOx-, and LOx-based mini-reactors, respectively, were disconnected. The same outcome was obtained for the ACh biosensor in the case of the absence of two mini-reactors as well as with only one AChE-mini-reactor (grey and black lines in **Fig. 3.2(B)**). However, the presence of the only ChOx-based mini-reactor (the AChE-based one was disconnected) gave a signal (bright green line in **Fig. 3.2(B)**), meaning that ACh undergoes spontaneous chemical hydrolysis (this phenomenon was previously reported in [109]). The peak height of ACh non-enzymatic hydrolysis was 10 % of the peak height attributed to enzymatic hydrolysis and it was always subtracted to estimate the response of the ACh biosensor (the used software allowed this to be done automatically). In general, no observed peaks while measuring without the enzymatic mini-reactors confirm that the downward peaks are related to enzymatic oxygen consumption and demonstrate the feasibility of the proposed biosensing platform.

All the steps in relation to the development of the four aforementioned biosensors, including the design of the AgA-based transducers, the preparation of the enzymatic mini-reactors, the optimization of the biosensors' operating parameters, the evaluation of the biosensors' analytical performance as well as the selectivity, reusability, and storage stability, and finally, their practical application in the analysis of the analyte-containing samples, are discussed separately in the following ***subchapters***.

3.1 Detection part – design of the silver amalgam-based transducers

3.1.1 Silver solid amalgam electrode covered by mercury film incorporated in the flow cell of wall-jet mode

The TD-p-AgSA, developed and constructed as part of O. Josypčuk's Ph.D. thesis (see ***subchapter 2.2***), was first among amalgam electrodes, successfully used as the detector for flow-through electrochemical biosensors [74]. Numerous previous electroanalytical studies performed in the batch arrangement, demonstrating that the use of m-AgSAE and MF-AgSAE as WEs is superior to p-AgSAE in terms of sensitivity [65, 121-123], prompted us to design MF-AgSAE with the intention of testing it as a transducer for the future amperometric biosensors in FIA. At the same time, the necessary flow cell was constructed, which works in the wall-jet mode.

The photo and scheme of the designed wall-jet cell along with the working MF-AgSAE are depicted in **Fig. 3.3**. In fact, the fabrication of the MF-AgSAE (a PEEK chromatographic capillary (ID 0.5 mm, OD 1.6 mm, length 40 mm, serving as the electrode body) consisted of preparing of the p-AgSAE and immersing it in liquid mercury. After 30 seconds of vigorous stirring, the electrode was gently tapped on the wall of a glass beaker to remove excess mercury so that it remained in the form of a thin film. The mercury films obtained in this way were reproducible and stable for at least the whole working day [124].

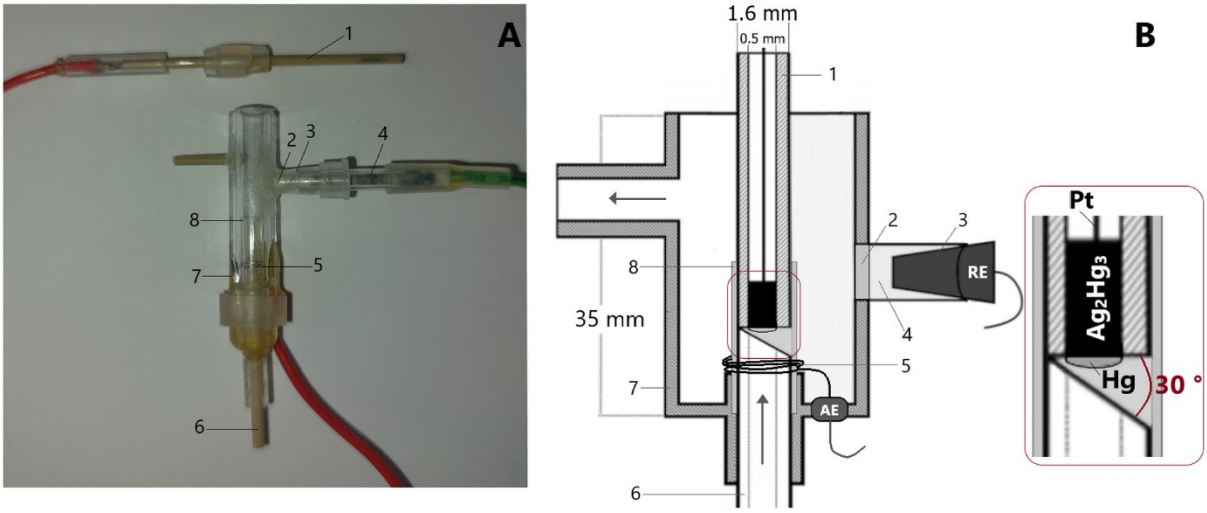

Fig. 3.3 The photo (**A**) and scheme (**B**) of the constructed three-electrode wall-jet cell: 1 − the working MF-AgSAE, 2 – filter paper, 3 − solution of the saturated KCl, 4 − reference electrode – saturated calomel electrode based on silver paste amalgam, 5 − auxiliary electrode – platinum wire, 6 – inlet PEEK capillary (ID 0.5 mm, OD 1.6 mm) cut off at an angle of 30 ° to the WE, 7 – Plexiglas® tube (ID 4.0 mm, OD 6.5 mm, length 35 mm), 8 − inner tube (ID 1.6 mm) cut in half lengthwise.

Next, the three-electrode wall-jet cell was constructed based on the Plexiglas® tube (ID 4.0 mm, OD 6.5 mm, length 35 mm, item 7 **in Fig. 3.3**). Apart from the prepared working MF-AgSAE (1), it incorporated an auxiliary platinum electrode (10 mm-long wire with a diameter of 0.2 mm, 5) and a miniaturized saturated calomel electrode based on silver paste amalgam (SCE-AgA, 4) as a reference one (SCE-AgA has the same potential as the classic SCE and was developed within O. Josypčuk's Ph.D. thesis [74]). To overcome the main challenge of the wall-jet cell, associated with the unreliable position of the WE, we proposed to cut the inlet capillary (6) obliquely. Such a simple technical solution ensured the WE was positioned always at the same distance from the inlet capillary. The angle at which the inlet capillary (ID 0.5 mm, OD 1.6 mm) should be cut off was optimized to be 30 º. Besides, to provide that the WE was placed strictly in the centre of the inlet capillary, the additional inner tube (ID 1.6 mm, length 15 mm, 8) cut in half lengthwise was fixed at the bottom of the Plexiglas® tube, into which the inlet capillary and MF-AgSAE are inserted.

Overall, the MF-AgSAE integrated into the wall-jet cell represents the miniature detector with a simple, robust, and inexpensive design that can be applied to monitor redox processes, especially those that require a strong negative potential.

Finally, the constructed MF-AgSAE coupled to the ChOx-based mini-reactor was used to develop the Ch biosensor [**115**]. In addition, for comparison, the Ch biosensor, where the TD-p-AgSA acted as the transducer, was investigated as well. In brief, as expected, the use of the MF-AgSAE provided a better result in terms of biosensor sensitivity compared to the TD-p-AgSA (see ***subchapter 3.4*** for more details).

Later, the MF-AgSAE was also utilized as a transducer for the ACh biosensor because the ACh determination required higher sensitivity [**116**]. Instead, the UA biosensor was developed using the TD-p-AgSA. Since sensitivity was not critical in the UA analysis, the choice of TD-p-AgSA was justified by the technical advantage of working in the flow-through cell used with this type of detector, *i.e.*, avoiding the issue of air bubbles. The problem of air bubbles associated with the different cell configurations is discussed below in ***subchapter 3.4***.

3.1.2 Silver amalgam screen-printed electrode

We have proposed a facile, rapid, and reliable technique for the preparation of the first AgA-SPEs, which is based on the automated and computer-controlled electrochemical deposition of mercury ions on the commercially available Ag-SPEs [**118**]. Consequently, the developed AgA-SPEs were found to be the perspective detectors with the substantial advantage of enabling electroanalysis of various compounds, especially, reducible at highly negative detection potentials not reachable using the original Ag-SPEs. It should be clarified that the Ag-SPE used is the three-electrode SPE composed of an Ag disc as a WE, a carbon auxiliary, and an Ag pseudo-reference electrode (pseudo-RE). As the auxiliary and reference electrodes did not undergo any transformations and remained the same, the denotation Ag-SPE used stands for the working Ag disc electrode on the SPE. Two commercially available Ag-SPEs with diameters of 1.6 or 4 mm, $Ag_{1.6}$-SPE and Ag_4-SPE, were used for mercury deposition, resulting in amalgam electrodes designated $AgA_{1.6}$-SPE and AgA_4-SPE, respectively.

To electrochemically deposit mercury ions at the Ag-SPE, the simple electrolyser was constructed (its scheme and photo are presented in *Appendices/**Publication IV**/Fig. 1)*. In fact, the designed electrolyser is a 10mL plastic syringe serving as its body, where the Ag-SPE was connected as a cathode, while the silver paste amalgam (12 % (*w/w*) Ag) at the bottom of the electrolyser acted as an anode. A solution of 0.1 mol L^{-1} HgO (for $AgA_{1.6}$-SPE) or 0.05 mol L^{-1} HgO (for AgA_4-SPE) in 2 mol L^{-1} KI was suggested as an electrolyte. A great advantage of this electrolyser configuration is the stability of the electrolyte solution. Since the amount of mercury ions deposited on the Ag-SPE is compensated by the same amount of mercury ions released from the anode into the solution, the electrolyte solution was not depleted. For instance, the same solution has already been used to prepare >200 AgA-SPEs so far.

As stated above, the procedure of the mercury electrodeposition was automated and computer-controlled. The charge required to deposit the calculated weight of mercury was loaded to the panel of the electrolysis parameters in the control software, upon reaching which the electrolysis was automatically stopped. To calculate the needed charge (number of micro-coulombs), the Faraday law was used assuming the current yield equals 100 %. The deposition was carried out at the pre-optimized potential value of −200 mV and lasted *ca.* 96 s for the $AgA_{1.6}$-SPE (current was maintained at about −550 μA) or 60 s for the AgA_4-SPE (current was around −900 μA). The mercury was deposited at the Ag-SPE surface in the form of numerous micro-droplets. It can be explained by the fact that the Ag disc is not a pure Ag, but is a

composite consisting of the Ag powdered particles that are glued by some nonconductive organic polymer (adhesive). Nevertheless, after immersing freshly prepared AgA-SPE in 0.2 mol L^{-1} KCl and applying a potential of −2000 mV (*vs.* SCE-AgA) for 20 s, which is a mandatory final step in the design of these electrodes, the mercury micro-droplets instantly merged, forming an even, smooth, and shiny surface. Over the next 1 – 2 h, mercury gradually impregnated the Ag particles, and dissolved them, turning into non-toxic AgA (the shiny electrode surface visually became matte).

In order to design AgA-SPE with the most favourable electrochemical and mechanical properties, it was necessary to optimize the amount of Hg that should be deposited on Ag-SPE. However, the Ag content of the Ag-SPE had to be identified originally, as the manufacturer does not provide this information. The amount of Ag in $Ag_{1.6}$-SPE was determined by differential pulse voltammetry (DPV) (the detailed procedure is given in *Appendices/**Publication IV**/section 3*) and calculated to be 56.3 ± 3.5 μg. The quantification of Ag in Ag_4-SPE was not experimentally performed. Instead, a value of 355 μg was taken, since the geometric surface area (A_{geom}) of Ag_4-SPE is 6.3 times larger than that of $Ag_{1.6}$-SPE.

Then, the different Hg amounts were deposited on the Ag-SPEs so that to prepare AgA-SPEs with Hg content from 10 to 80 (*w/w*)). First of all, the potential of the hydrogen evolution (PHE) on AgA-SPEs was found to be significantly dependent on the Hg amount deposited for electrode preparation (the corresponding dependence is presented in *Appendices/**Publication IV**/Fig. 3*). Specifically, for AgA-SPEs of both diameters, the gradual increase in Hg content caused considerable shift of the PHE, measured in 0.1 mol L^{-1} NaOH, to more negative values, reaching it maximum at 50 % (*w/w*) of Hg. With the further increase in Hg content, the PHE remained practically constant. As shown in **Table 3.2**, the PHE values in 0.1 mol L^{-1} NaOH for AgA-SPEs with 50 % (*w/w*) of Hg are notably more negative (by 387 and 363 mV for the $AgA_{1.6}$-SPE and AgA_4-SPE, respectively) than those for the original Ag-SPEs, indicating the wider potential windows for the prepared amalgam electrodes. A similar phenomenon, more negative PHE values on AgA-SPE compared to those on Ag-SPE, was also obtained in neutral and acidic media, although, in the latter, the difference was less explicit (see **Table 3.2**).

Table 3.2 The PHE values on the prepared AgA-SPEs (50 % (*w/w*) of Hg) and the original Ag-SPEs. Uncertainty represents standard deviation (SD) for seven repeated measurements.

Electrode	The potential of hydrogen evolution (PHE) / mV [(a)]		
	0.1 mol L^{-1} HCl	0.1 mol L^{-1} phosphate buffer, 1.0 mmol L^{-1} Na_2EDTA, pH 6.5	0.1 mol L^{-1} NaOH
$AgA_{1.6}$-SPE	n.d. [(b)]	n.d.	−1979 ± 4
$Ag_{1.6}$-SPE	n.d.	n.d.	−1592 ± 12
AgA_4-SPE	−885 ± 3	−1527 ± 5	−1896 ± 10
Ag_4-SPE	−784 ± 2	−1152 ± 6	−1533 ± 2

Abbreviation: Na_2EDTA – disodium ethylenediaminetetraacetate.

[(a)] The PHE values correspond to 10.0 and 62.5 μA current levels for the SPEs with the diameter of the working Ag or AgA disc electrode of 1.6 and 4 mm, respectively.

[(b)] Not determined.

It is worth noting that the AgA-SPEs, where the Hg content was ≥70 % (*w/w*), were not mechanically stable, as the amalgam disc was fragile or paste and could be easily peeled off from the ceramic support after one day. Thus, based on the above results, it is recommended to prepare $AgA_{1.6}$-SPE and AgA_4-SPE with 50% (*w/w*) Hg content, which means deposition of 56.3 and 355 μg of Hg on $Ag_{1.6}$-SPE and Ag_4-SPE, respectively (these electrodes were used for all further experiments).

Next, electrochemical characteristics of the constructed AgA-SPEs were obtained from cyclic voltammetry measurements of outer-sphere $[Ru(NH_3)_6]^{3+/2+}$ redox marker at the scan rates in the range from 10 to 500 mV s^{-1}. Analysing a recorded pair of the redox peaks of $[Ru(NH_3)_6]^{3+/2+}$, it can be concluded that AgA-SPEs meet three reversibility criteria: (i) closeness of the cathodic peak-to-anodic peak separation to the theoretical value of 59 mV, (ii) approaching of the peak current ratio to 1, and (iii) linear relationship between the peak current and the square root of the scan rate (all data are summarized in *Appendices/**Publication IV**/Table 1*). Similar outcomes were obtained for the original Ag-SPEs, indicating fast electron transfer kinetics and high quality of both types of SPEs. Regarding the effective surface area (A_{eff}), it was calculated using the Randles-Sevcik equation [125] and estimated to be 1.6 mm^2 for $AgA_{1.6}$-SPE and 9.3 mm^2 for AgA_4-SPE, meaning that 80 and 74 % of their A_{geom}, respectively, are truly accessible for electrochemical processes. The values are consistent with those for the original Ag-SPEs (see *Appendices/**Publication IV**/Table 1).* An analogous discrepancy between A_{eff} and A_{geom} is also reported for other SPEs and attributed to the presence of some nonconductive binder [126].

Further, to verify the practical applicability of the fabricated electrodes, the $AgA_{1.6}$-SPE was tested for the determination of iodate (IO_3^-) in the table salt by employing DPV (pulse height was −50 mV, scan rate 20 mV s^{-1}, supporting electrolyte [0.1 mol L^{-1} NaOH; 1.7 mol L^{-1} NaCl]). The IO_3^- determination is based on its electrochemical reduction to iodides (I^-) at the highly negative potential. It is immediately evident from **Fig 3.4(A)** that at $Ag_{1.6}$-SPE, there is only a hint of a peak over −1200 mV (*vs.* Ag pseudo-RE), moreover, close to the supporting electrolyte decomposition, which is unlikely to be applied for analytical determination because of the difficulty of its evaluation. In contrast, a well-defined peak at −1072 mV (*vs.* Ag pseudo-RE) was recorded at $AgA_{1.6}$-SPE, which clearly demonstrates the advantage of amalgam electrodes, namely their use for reduction processes that occur at highly negative potentials. Apart from that, the lower background current and, as expected, the substantially shifted PHE to more negative values are obvious at $AgA_{1.6}$-SPE. The found amount of IO_3^- per 1 kg of table salt, 25.3 ± 1.9 mg, well agrees with the manufacturer's declared value (27 ± 7 mg kg^{-1}). Notably, statistically similar results, 27.3 ± 1.0 mg, were obtained with five independently prepared $AgA_{1.6}$-SPEs, confirming the high reproducibility of the amalgam SPE fabrication procedure as well as the reliability of the analysis using them as WE.

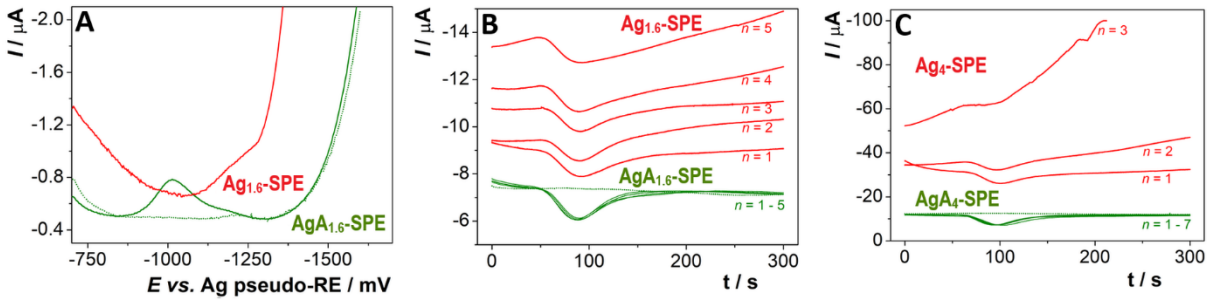

Fig. 3.4 DPVs recorded on $Ag_{1.6}$-SPE (red) and $AgA_{1.6}$-SPE (green) for the IO_3^- determination in the table salt (**A**). Amperograms of the LA determination using the biosensor consisting of the LOx-based mini-reactor coupled either to $Ag_{1.6}$-SPE (**B**, red), $AgA_{1.6}$-SPE (**B**, green), Ag_4-SPE (**C**, red), or AgA_4-SPE (**C**, green) as a transducer (LA concentration (c_{LA}) 500 µmol L^{-1}, detection potential (E_{det}) = −1100 mV *vs.* Ag pseudo-RE, v_{flow} = 0.1 mL min^{-1}, $V_{inj,\,LA}$ = 40 µL, CS [0.1 mol L^{-1} phosphate buffer, 1.0 mmol L^{-1} disodium ethylenediaminetetraacete (Na_2EDTA), pH 6.5], *n* – serial number of measurement).

At last, the AgA-SPEs, as well as Ag-SPEs for comparison, were tested as potential biosensor transducers. For this purpose, they were alternately connected to a LOx-based mini-reactor and used to determine LA by monitoring the four-electron reduction of the enzymatically consumed oxygen at −1100 mV *vs.* Ag pseudo-RE. As depicted in **Fig. 3.4(B, C)**, the well-repeatable amperograms ($n \geq 5$) with a downward peak were recorded using AgA-SPEs as the transducer. On the contrary, in the case of Ag-SPE, the obtained amperograms were substantially distorted, which is undoubtedly associated with the closeness of the detection potential to the PHE. The longer the detection potential was applied to Ag-SPEs, the more hydrogen microbubbles were formed (visible to the naked eye), which led to an impairment of the amperogram recording with each subsequent measurement. Thus, it can be concluded that AgA-SPEs, unlike Ag-SPEs, can be used as biosensor transducers for monitoring four-electron oxygen reduction (Ag-SPEs can be utilized to measure enzymatically consumed oxygen, but the peak current can be 2 times lower, which will negatively affect the sensitivity).

In general, the simple and rapid preparation procedure together with satisfactory electrochemical performance and suitability for use at high negative potential make AgA-SPEs promising electrodes in (bio)electroanalysis.

Based on the more convenient signal-to-background ratio, the fabricated $AgA_{1.6}$-SPE incorporated into the commercially available wall-jet cell for the SPEs was selected for further development of the LA biosensor. It should be emphasized that despite the concept of disposable-use SPEs, all measurements were performed with a single $AgA_{1.6}$-SPE, as no electrode fouling was observed (see ***subchapter 3.7*** for more details).

3.2 Biorecognition part – preparation of the enzymatic mini-reactor

3.2.1 Comparison of the different supports and covalent techniques for enzyme immobilization

As enzyme immobilization methods, we preferred covalent binding due to the formation of a strong bond in the enzyme-support conjugate. Given the different covalent protocols can contribute to various amounts of bound enzyme, its properties and, in turn, different biosensor characteristics [127], finding the most suitable one was a primary task to create the most efficient enzyme mini-reactors. Since a broad comparison of different approaches to covalent immobilization is associated with high enzyme consumption, this study was performed using GOx [128] and Lac [**119**], chosen as test enzymes because of their affordability.

In the beginning, three well-known techniques based on the use of two different activation agents, GA (technique *A*) and *N*-(3-dimethylaminopropyl)-*N*′-ethylcarbodiimide/*N*-hydroxy-succinimide (EDC/NHS), the latter in its two variants (techniques *B* and *C*), were investigated for the glucose oxidase (GOx) and laccase (Lac) immobilization utilizing two MSP representatives, MCM−41 and SBA−15, as support:

(i) technique *A* − enzyme attachment by its $-NH_2$ groups to $-NH_2$ functionalized support *via* GA, producing a covalent secondary amine bond,

(ii) technique *B* – enzyme coupling by its –COOH groups activated by EDC/NHS to $-NH_2$ functionalized support with the derivation of a covalent amide bond .

(iii) technique *C* – enzyme attachment by its $-NH_2$ groups to –COOH functionalized support activated by EDC/NHS, forming a stable amide bond [127].

The immobilization procedure for each technique, which basically includes three consecutive steps (the formation of the functional groups on support, activation of either the support (techniques *A* and *C*) or the enzyme (technique *B*) groups, and the actual attachment of the enzyme), is described in detailed in *Appendices/**Publication IV**/Supplementary material.* For the synthesis of $-NH_2$ and –COOH functional groups on MCM−41 and SBA−15, the silanization method was applied. Accordingly, MSPs were treated with APTES and CEST solutions, which led to their coating with aminopropyl and carboxyethyl moieties, respectively

It was found that both the GOx- and Lac-based biosensors were highly dependent on the technique of enzyme immobilization used, and as shown in **Fig. 3.5**, the responses to 0.5 mmol L^{-1} of glucose or 0.5 mmol L^{-1} of dopamine, respectively, decreased in the next order: technique *A* → technique *B* → technique *C*. This tendency was observed on both MSPs.

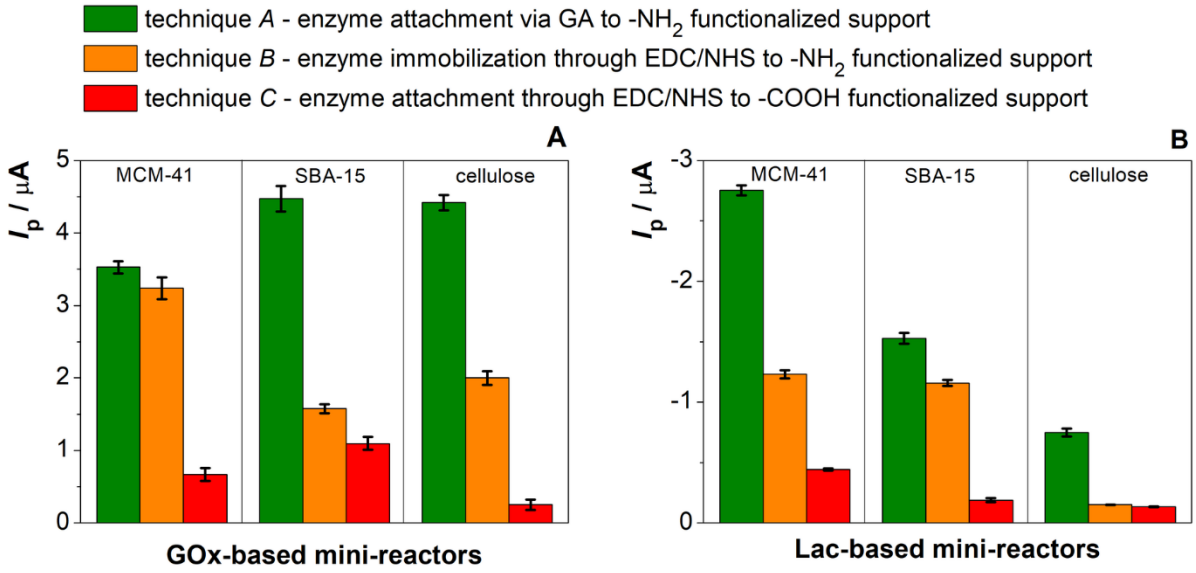

Fig. 3.5 Effect of three covalent immobilization techniques and types of support used for the preparation of GOx- (**A**) and Lac-based (**B**) mini-reactors on the biosensor responses. *Experimental conditions:* (A) $c_{glucose}$ = 0.5 mmol L^{-1}, E_{det} = −1100 mV, v_{flow} = 0.1 mL min^{-1}, $V_{inj,\ glucose}$ = 40 µL, CS: [0.1 mol L^{-1} acetate buffer (AcB), 1.0 mmol L^{-1} Na_2EDTA, pH 6.5]; (B) $c_{dopamine}$ = 0.5 mmol L^{-1}, E_{det} = −50 mV, v_{flow} = 0.1 mL min^{-1}, $V_{inj,\ dopamine}$ = 40 µL, CS: [0.1 mol L^{-1} AcB, pH 4.8]. Error bars are estimated as standard deviation (SD) of five consecutive measurements.

Such results were suggested to be originated from the following factors affecting enzyme binding:

(1) Differences in the stability and reactivity of GA and EDC/NHS as well as their intermediates resulted in the activation step. Comparing to the GA-activated support, which is reported to be highly stable (it does lose the ability to interact with $–NH_2$ groups for at least 24 h [129]), the ester formed after the activation of –COOH group by EDC/NHS exists only for a short period (around 1 h [130]), leading to the time-limited interaction between the enzyme and support (if the EDC/NHS activated –COOH group does not find and react with the target $–NH_2$ group during its lifetime, it hydrolyses and the necessary attachment does not occur).

(2) Difference in the distance between the enzyme and support. In contrast to zero-length EDC/NHS, GA with a 5-atom spacer arm may ensure a wider range of angles for the reaction of the enzyme with aminated support, thereby facilitating immobilization. Besides,

according to aldol condensation, GA can exist as the oligomeric molecules (dimeric or trimeric) in the aqueous media, which may lead to an even longer distance between the enzyme and support, resulting in much lower steric hindrances for enzyme binding [131].

(3) Difference in the density of functional groups formed at the support surface. The higher the content of support functional groups, the higher the probability of enzyme attachment. As shown in **Table 3.3**, the amounts of aminopropyl and carboxyethyl moieties covered on, for example, 1 g of MCM−41 were calculated to be 4.47 ± 0.09 and 2.63 ± 0.11 mmol g^{-1}, respectively, which means 1.7 times higher content of $-NH_2$ groups compared to −COOH ones.

Additionally, in technique *B* based on the interaction of the EDC/NHS with the enzymatic –COOH groups, it may come to the polymerization/aggregation of the enzyme molecules, *i.e.*, considering the presence of both free $-NH_2$ and −COOH groups on the enzyme surface, the activated −COOH group on one enzyme molecule can crosslink with $-NH_2$ group of another enzyme molecule. It should be noted that this effect can cause both an increase (binding of large enzyme aggregates to the support) and a decrease in the amount of immobilized enzyme (lack of time for the short-lived activated −COOH group of the enzyme to react with the $-NH_2$ group on the support surface after it has spent time reacting with the $-NH_2$ group of another enzyme).

Table 3.3 Quantities of alkylsilane moieties with different functional groups ($-NH_2$, −COOH, and −epoxy) anchored to various types of supports, MSPs (MCM−41 and SBA−15) and cellulose. Uncertainty represents SD for three repeated measurements.

Precursor silane compound	**Functional group**	**Amount of the attached amino-, carboxy-, and epoxyalkylsilane moieties per 1 g of the support / mmol g^{-1}**		
		MCM−41	SBA−15	cellulose
APTES	$-NH_2$	4.47 ± 0.09	4.36 ± 0.10	0.269 ± 0.024
AEAPTMS [(a)]	$-NH_2$	2.52 ± 0.071	1.72 ± 0.081	n.d. [(d)]
AEAEAPTMS [(b)]	$-NH_2$	1.94 ± 0.02	1.41 ± 0.040	n.d.
CEST	−COOH	2.63 ± 0.11	n.d.	0.273 ± 0.013
GOPTES [(c)]	−epoxy	n.d.	0.72 ± 0.06	n.d.

[(a)] [3-(2-aminoethylamino)propyl]trimethoxysilane
[(b)] 3-[2-(2-aminoethylamino)ethylamino]-propyltrimethoxysilane
[(c)] (3-glycidyloxypropyl)trimethoxysilane
[(d)] Not determined

Judging from the factors above-mentioned, it is relevant to assume that the lowest biosensor responses attained using the technique *C* might be associated with the lowest amounts of immobilized enzymes, which reasonably follows from the unfavourable coupling conditions, such as the low stability of the activated support, the shortest distance in the enzyme−support conjugate (determined by the length of the carboxyethyl moieties), and lower content of −COOH functional groups grafted to the support. Meanwhile, the high stability of the GA-activated support along with the providing distance between the enzyme and support, and the higher content of the support $-NH_2$ functional groups could have collectively resulted in the highest degree of enzyme loading by technique *A* and, consequently, the highest biosensor response.

Addressing the comparison of the two types of MSPs *via* the GA technique (see **Fig. 3.5**, green bars), it could be seen that for the Lac-based biosensor, a higher response was obtained utilizing MCM−41 compared to SBA−15, *i.e.,* 1.7 times, which correlates well with the surface area of these MSPs (see ***subchapter 2.2***), while in the case of GOx, this difference is not so noticeable. Since GOx activity is higher than Lac activity (*ca.* 10 times comparing the data for free enzymes), it is reasonable to claim that the overall activity of a GOx-based mini-reactor, determined by the enzyme loading, is less dependent on the support surface area (*i.e.,* even if less GOx is immobilized on SBA−15 due to its smaller surface area, it is still sufficient for efficient enzymatic conversion).

Then, the immobilization of GOx and Lac by these three covalent techniques was tested on the cellulose powder, the selection of which was justified by its lower price compared to MSPs. Furthermore, a cellulose powder with a larger particle size (20 μm) than MCM−41 (2.1 − 2.7 μm) and SBA−15 (2 − 6 μm) was specifically selected to test whether it was possible to achieve higher sample throughput by operating at higher flow rates. It should be mentioned that the same silanization procedure was employed for the synthesis of $-NH_2$ and −COOH functionalized cellulose as for MSPs. As demonstrated in **Table 3.3**, it was found that the notably lower quantity of both functional groups was attached to the surface of cellulose powder compared to MSPs (*e.g.,* decrease in the content of $-NH_2$ and −COOH groups by 16.6 and 9.6 times, respectively, in comparison to MCM−41), which is conditioned by its smaller surface area and lower density of the surficial −OH groups. However, unlike MSPs, the amounts of aminopropyl and carboxyethyl moieties attached to cellulose are relatively similar. In regard to the comparison of three covalent immobilization techniques, the same phenomenon as for MSPs was clearly observed on the cellulose support for both enzymes, *i.e.*, the highest biosensor responses were recorded when technique *A* was used for enzyme immobilization, whereas

intermediate and lowest ones were obtained with techniques *B* and *C*, respectively, as depicted in **Fig. 3.5**. However, comparing the results for technique *A*, in the case of Lac, a 3.7-fold lower signal was recorded using cellulose than MCM−41, while for GOx, the biosensor responses are almost comparable. This revealed that not only the surface area of the support but also the degree of its functionality is more important for the immobilization of Lac than GOx. In addition, it is worth noting that the maximum flow rate that can be operated with the cellulose-filled mini-reactors is 0.8 mL min^{-1}, due to less compression of the larger particles in the mini-reactor, resulting in the lower hydrodynamic resistance in the FIA system and providing higher sample throughput (this is twice that of the MSPs-filled mini-reactors).

Next, the third type of support, carbonaceous powders, including glassy carbon (GC) and graphite (Gr), was tested. This type of investigation was performed only for Lac. Besides, only two techniques *A* and *C* were chosen for comparison, as the GA technique appeared to be the most favourable based on our previous studies described above, while the enzyme attachment through EDC/NHS on –COOH groups of the support surface is reported to be the most frequently applied protocol for this type of support [132]. Concerning the formation of the functional groups on GC and Gr, −COOH groups were attained by classic chemical oxidation of their surfaces with a mixture of concentrated mineral acids H_2SO_4 and HNO_3, whereas the synthesis of $-NH_2$ groups was carried out by employing two different approaches: (i) silanization with APTES after the preliminary formation of −OH groups and (ii) diazonium salt chemistry using 1,4-diaminobenzene (procedures and preparation schemes are presented in *Appendices/**Publication V**/Supplementary material*).

As a result, the tendency of more favourable attachment of Lac by technique *A* in comparison to technique *C*, true for both carbon-based powders, was observed as well (see *Appendices/**Publication V**/Fig. 3*). However, contrary to two former types of support investigated, a significantly high contribution of physical adsorption was observed, especially in the case of technique *C*. The biosensors with the mini-reactors based on the Lac physically adsorbed at the carboxylated GC and Gr exhibited the peak currents, which made up 87.5 and 64.7 %, respectively, of the signals obtained with the appropriate mini-reactors where Lac was covalently attached to the same supports through EDC/NHS. Such behaviour suggests that the adsorption of Lac at the carbonaceous support, due to its spontaneity, is the dominating process over the much slower covalent reactions, indicating the importance to differentiate the covalent attachment from adsorption in the immobilization mechanism. Gao *et al*. generally question the efficiency of enzyme immobilization with EDC/NHS on the −COOH functionalized

carbon support, as it has also been observed for other enzymes that EDC can only marginally improve immobilization compared to the adsorption level [133].

Regarding the comparison of the two synthesis approaches of $-NH_2$ groups at GC and Gr, higher biosensor responses were observed using diazonium salt chemistry over silanization. Assumedly, the inferior signals when the silanization was used could be attributed to the lower content of the $-NH_2$ groups formed, since the grafting of the 4-aminobenzyl radicals (diazonium salt chemistry) occurs directly at the carbon surface, while the anchoring of the aminopropyl moieties (silanization approach) is additionally determined by the efficiency of the previous support functionalization by –OH groups. Nevertheless, although covalent Lac immobilization *via* GA to the 4-aminobenzyl-functionalized Gr proved to be the most suitable protocol among all tested for carbonaceous support, the resulting biosensor response was still inferior to that obtained with the mini-reactor consisting of Lac covalently attached to aminated MCM−41 *via* GA.

After identifying the most appropriate crosslinking agent (GA, technique *A*) and type of support (MSP, particularly MCM−41), the Lac immobilization protocol was subjected to further experiments, which included testing, apart from APTES (3 atoms between the central Si atom and the functional $-NH_2$ group), two other longer aminoalkylsilanes, such as [3-(2-aminoethylamino)propyl]trimethoxysilane (AEAPTMS, 6 atoms) and 3-[2-(2-aminoethylamino)ethylamino]-propyltrimethoxysilane (AEAEAPTMS, 9 atoms) to obtain the most effective amino-functionalized MCM−41. As shown in **Table 3.3**, the use of AEAPTMS and AEAEAPTMS resulted in a 1.8- and 2.3-fold decrease, respectively, in the number of $-NH_2$ groups attached to the MCM−41 compared to APTES. To put it simply, the longer the aminosilane, the worse the coverage degree of MCM−41 by the $-NH_2$ groups, which is most likely due to increased steric hindrance. However, despite this fact, an enhancement in the amount of immobilized enzyme was observed. As determined by the Bradford method, 646, 787, and 893 μg of Lac were attached at 50 mg of aminated MCM−41 prepared using APTES, AEAPTMS, and AEAEAPTMS, respectively (the general principle, as well as the procedure for determining the amount of immobilized enzyme by the Bradford spectrophotometric method [134] is described in *Appendices/**Publication V**/Supplementary material*). Thus, these outcomes demonstrated that in this case, the longer distance in the enzyme−support conjugate, allowing a wider range of attachment angles and less steric hindrance, was a more dominant factor ruling the efficiency of enzyme immobilization than the number of grafted functional groups. Nevertheless, in spite of our expectations of achieving higher biosensor stability owning to the higher enzyme loading, the biosensors with mini-reactors based on all three

aminoalkylsilanes, APTES, AEAPTMS, and AEAEAPTMS, exhibited relatively similar responses, 47.9, 44.5, and 53.7% of the initial value, respectively, after regular use every 7 – 10 days for 4 months. It can be assumed that the increased mobility of longer aminoalkylsilanes and, consequently, the lower stiffness of the enzyme−support conjugates may cause a negative effect associated with the more significant conformational changes in the tertiary enzyme structure explaining the lack of a noticeable improvement in biosensor stability [135].

Next, we found it is noteworthy to investigate the application of another amine reactive homobifunctional cross-linking reagent DSS with 8-atom spacer instead of 5-atom GA for the Lac attachment. For comparison, the aminated MCM−41 supports prepared with the three above-mentioned aminoalkylsilanes were also used. Schematic illustrations of the respective enzyme−support conjugates are provided in *Appendices/**Publication V**/Fig. 5*. By contrast to GA, in the case of disuccinimidyl suberate (DSS), the longer the length of aminoalkylsilanes used, the lower the content of the attached Lac. In particular, 414, 268, and 110 μg of Lac, determined by the Bradford method, were covalently coupled *via* DSS to the 50 mg MCM41-NH_2 obtained by the use of APTES, AEAPTMS, and AEAEAPTMS, respectively. This deterioration of Lac immobilization may be due to the fact that the amount of DSS able to bind to the enzyme decreases with increasing aminosilane length. In other words, the longer the aminosilane, the higher probability that DSS will react with its second end with another free $-NH_2$ group at the MCM−41 surface. Thus, if both ends of the DSS will react with support, the possible sites for enzyme immobilization are decreased. Such change in the enzyme loading naturally manifested itself in the obtained responses of the biosensor to 0.5 mmol L^{-1} dopamine, where the highest peak current of 2.0 μA was acquired in the case of APTES, while the peak current decreased by a factor of 1.2- (AEAPTMS) and 1.7 (AEAEAPTMS). In addition, these signals are lower than those obtained using GA as the crosslinker (see *Appendices/**Publication IV**/Fig. 5*). This difference may be caused by the difference in the densities of the crosslinking agents coupled to the aminated MCM−41 and/or their reactivity (despite both crosslinking agents are amine-reactive, GA is *bis*-ahdehyde, while DSS contains NHS esters). In addition, the different mechanisms of bond formation might also lead to the different properties of the immobilized Lac, which resulted in different biosensor responses.

In the light of the interpreted results, it can be argued that the immobilization with GA on aminated MSPs (prepared with APTES) for both tested enzymes, GOx and Lac, is the most favourable, as the corresponding mini-reactors provided the best biosensor sensitivity and stability. Last, but not least, it should be pointed out that the enzyme attachment *via* this protocol

is straightforward and time-saving. In our laboratory, it was found that animated MSPs might be stored in the refrigerator at 4◦C for at least 2 years without losing their properties. Hence, once the SBA15-NH_2/MCM41-NH_2 is prepared, the entire procedure of the enzymatic powder preparation lasts only 3 h.

*Biosensor characteristics, including storage stability, detection limit (for dopamine), and measurement repeatability, obtained with all twenty Lac-based mini-reactors constructed within this comparative study, along with the total time required to prepare each mini-reactor, are summarized in Appendices/**Publication IV**/Table 2.*

3.2.2. Optimization for the target enzymatic mini-reactors

Based on the previous results, the GA-technique and APTES-treated MSPs as supports were chosen for the immobilization of the target enzymes − ChOx, AChE, UOx, and LOx.

Accordingly, two enzymatic powders, *i.e.*, the aminated SBA−15 and MCM−41 covalently coated with ChOx using GA, were packed in two Plexiglas® tubes (ID 4 mm), and the resulting two enzymatic mini-reactors (ChOx−SBA15-$NH_{2\ (GA)}$ and ChOx−MCM41-$NH_{2\ (GA)}$) were tested to select the best one. Analogously, the same set of two mini-reactors was prepared with LOx, LOx−SBA15-$NH_{2\ (GA)}$ and LOx−MCM41-$NH_{2\ (GA)}$. For both enzymes, the two mini-reactors, regardless of the support type, provided comparable biosensor responses, demonstrating the possibility of using any of tested MSPs (results for LOx are presented in *Appendices/**Publication VI**/Fig. 2*). Due to the slightly lower price of SBA−15, ChOx−SBA15-$NH_{2\ (GA)}$ and LOx−SBA15-$NH_{2\ (GA)}$ mini-reactors were further selected as the biorecognition part for the Ch and LA biosensors, respectively.

For the ACh biosensor, the AChE−SBA15-$NH_{2\ (GA)}$ mini-reactor was constructed and utilized in tandem with the earlier prepared ChOx−SBA15-$NH_{2\ (GA)}$ mini-reactor (for convenience, the AChE was also attached to the SBA−15, as it was chosen for ChOx). Here, to achieve the best biosensor signal, two parameters were investigated: (i) the ratio of concentration of enzyme solutions and (ii) the configuration of the biorecognition part.

Since ChOx has a lower binding affinity to Ch (apparent Michaelis-Menten constant ($K_M^{\ app}$) is 2.84 mmol L^{-1}) than AChE has to ACh ($K_M^{\ app}$ = 0.0739 mmol L^{-1}), it was obvious that ChOx is a limiting enzyme in this AChE-ChOx bienzyme system. To put it simply, a lower

content of immobilized AChE compared to ChOx is needed to ensure the course of cascade enzymatic reactions. As expected, the maximum signal of the ACh biosensor was still achieved when the AChE-based mini-reactor was prepared using the AChE solution with the concentration of 0.83 U, which was 20-fold lower than the ChOx concentration used to prepare the ChOx mini-reactor. Further decrease of AChE concentration, in particular, by 50 and 100 times in comparison to ChOx, caused a drop in biosensor responses by 31.9 and 52.6%, indicating insufficient AChE loading (see *Appendices/**Publication II**/Fig. 3*). Therefore, to achieve the highest response of the AChE biosensor, the rule that the concentration of the AChE solution can be at most 20 times lower compared to the concentration of the ChOx solution was followed when designing the two cascade mini-reactors.

According to the configurations of the biorecognition part, in addition to the one described above, that is, two independent mini-reactors (separately prepared enzyme powders placed in two Plexiglas® tubes) (*1*), three more options (configurations *2*-*4*) were investigated: the separately prepared two enzymatic powders were packed (*2*) in one Plexiglas® tube as two segments spatially segregated with the cotton band of 1 mm, or (*3*) in one Plexiglas® tube previously being well-mixed, and (*4*) one enzymatic powder was prepared by the simultaneously covering of one SBA15-NH_2 portion with two enzymes using the solution of their mixture (for better visualization see the corresponding scheme in *Appendices/**Publication II**/Fig. 1*). It was anticipated that ensuring close contact between two enzymes (configurations *3* and *4*) or shortening the distance between the enzymatic powders (configuration *2*) would result in an enhancement of the biosensor response because the higher local concentration of the first product, due to the elimination of additional dilution, would lead to an increase in the rate of the second enzymatic reaction [136]. However, despite our expectations, the biosensor responses without any improvements were recorded; in other words, the investigated types of configurations did not affect either the height or even the width of the obtained peak. Although the enzymes co-immobilization approach (configuration *4*) simplifies the mini-reactor preparation (it is necessary to cover one portion of SBA15-NH_2 simultaneously instead of the preparation of two enzymatic powders), we preferred to work with two independently prepared mini-reactors (configuration *1*) because the easy disconnection of the AChE−SBA15-$NH_{2\ (GA)}$ mini-reactor changes the type of biosensor from the ACh detection to Ch detection.

Additionally, in order to reduce the cost of the ACh biosensor, an attempt was made to replace AChE with the more affordable enzyme, Esterase from *porcine liver* (Es). For this purpose, the mini-reactor based on the covalently immobilized Es *via* GA to SBA15-NH_2 (Es−SBA15-$NH_{2\ (GA)}$) was constructed. Although the ACh is an ester of acetic acid and choline

and Es is reported to have wide substrate specificities [137], the use of the Es−SBA15-$NH_{2\,(GA)}$ mini-reactor connected to ChOx−SBA15-$NH_{2\,(GA)}$ one gave a negligibly low signal of 0.5 mmol L^{-1} ACh. Even the pre-incubation of free Es (162 U) with ACh in the solution for 30 min, did not lead to a noticeable improvement, meaning that Es poses a low specificity for ACh hydrolysis. Based on this result, it can be claimed that the Es/ChOx bienzyme system is not suitable as the biorecognition element for the amperometric ACh biosensor.

With respect to choosing the most suitable UOx-based mini-reactor for the UA biosensor, some extended comparative study was performed. First of all, it should be pointed out that in order to estimate the effect of the enzyme source, all experiments were carried out for two kinds of UOx, in particular from *Candida species* (UOx(*C*)) and from *Bacillus fastidiosus* (UOx(*B*). Apart from technique *A* based on GA, both kinds of UOx were immobilized through EDC/NHS on the aminated SBA−15 (above-mentioned technique *B*) and directly on epoxy-functionalized SBA−15 prepared using (3-glycidyloxypropyl)trimethoxysilane (GOPTMS, technique *D*). The latter technique was not included in the comparative studies for GOx and Lac attachment because these enzymes according to the pH ranges of their stability (4−7 for GOx and 5.5−7.5 for Lac), unlike UOx (8.0−9.5), could be denatured in an alkaline medium (pH 9), which must be maintained for coupling to occur [130].

For both kinds of UOx, it was found that the covalent techniques used for the enzyme immobilization had the major influence and the biosensor responses to 500 μmol L^{-1} UA decreased in the following order: technique *A* → technique *B* → technique *D* (see *Appendices/**Publication III**/Fig. 2*), demonstrating the GA-coupling to be the most efficient, like in the cases of GOx and Lac. The lowest biosensor response acquired using technique *D* is most likely due to a substantially lower amount of the epoxy groups covering the SBA−15 surface compared to $–NH_2$ groups, namely 6.1 times (see **Table 3.3**), which provided a much lower enzyme loading. By comparing two MSPs, it was shown that both kinds of UOx were preferably immobilized at MCM−41 over SBA−15, providing slightly higher biosensor responses (see *Appendices/**Publication III**/Fig. 3*).

Regarding the effect of the enzyme type, no difference in the biosensor responses to 500 μmol L^{-1} UA using the UOx(*C*)−MCM41-$NH_{2\,(GA)}$ mini-reactor and the UOx(*B*)−MCM41-$NH_{2\,(GA)}$ mini-reactor was indicated, even though the activity of free UOx(*B*) is approximately 4.5 times higher than that for UOx(*C*). It can be assumed that if there is a difference between the total catalytic activity of both mini-reactors, it is so insignificant that it is not reflected in the biosensor signal. The UOx(*B*)−MCM41-$NH_{2\,(GA)}$ mini-reactor was selected as the biorecognition part.

Finally, it should be mentioned that the height of the enzymatic mini-reactor (H_r, in other words, the height of the enzymatic powder pressed into the Plexiglas® tube) was investigated. As a result, balancing between providing high biosensor sensitivity, large enzyme capacity in the mini-reactor, short measurement time, and low hydrodynamic resistance in the flow system, the H_r of 5 mm was selected as a compromise. This study was carried out with the ChOx-based mini-reactor, which was chronologically the first one prepared (for more details see *Appendices/**Publication I**/section 3.2.4*). Then, the obtained result was applied to prepare other target mini-reactors, as the Plexiglas® tubes with the same ID (4 mm) were always used.

3.2.3 Determination of the immobilized enzyme amount

The total quantity of the immobilized enzyme at the GA-activated $-NH_2$ functionalized either SBA−15 (for ChOx and LOx) or MCM−41 (for UOx(*B*)) was determined as the difference between the values of its initial amount in the solution taken for immobilization (listed in **Table 3.4**) and the residue remaining after it, which was found by Bradford method.

Table 3.4 Results regarding the enzyme loading at the MSPs using the covalent coupling with GA

	Enzyme		
	ChOx	**LOx**	**UOx(*B*)**
Enzyme amount in 1mL solution taken for immobilization / μg (U)	1720 (23.7)	950 (42.8)	2390 (21.5)
Immobilization efficiency[(a)] / %	81.9	85.3	79.9
Amount of the immobilized enzyme in μg per 1 mg of support[(b)]	28.6 ± 0.5	16.2 ± 0.1	40.6 ± 0.5
Amount of the immobilized enzyme in one mini-reactor	*ca.* 476	*ca.* 270	*ca.* 955

(a) Percentage ratio of the immobilized enzyme amount (μg) to the enzyme amount (μg) taken for the immobilization

(b) Either $-NH_2$ functionalized SBA−15 (for ChOx and LOx) or MCM−41 (for UOx(*B*))

Accordingly, 1427 ± 23 μg of ChOx and 810 ± 5 μg of LOx were estimated to be bound *via* GA to 50 mg of SBA15-NH_2. These results demonstrate the achieved high immobilization efficiency, as >80% of each enzyme was attached (see **Table 3.4**). Since such a portion of the enzymatic powder was sufficient to fill three Plexiglas® tubes resulting in three enzymatic mini-

reactors (H_r of each was 5 mm), it can be assumed that one ChOx−SBA15-$NH_{2\,(GA)}$ mini-reactor contains *ca.* 476 μg of the immobilized ChOx, while one LOx−SBA15-$NH_{2\,(GA)}$ mini-reactor contains *ca.* 270 μg of the immobilized LOx. In the case of UOx(*B*), 1910 ± 28 μg was bound to 47 mg of MCM41-NH_2, and the final enzyme amount in the UOx(*B*)−MCM41-$NH_{2\,(GA)}$ mini-reactor was estimated to be approximately 955 μg (the enzymatic powder prepared by taking 47 mg of the aminated MCM−41 is enough to fill only two Plexiglas® tubes with the H_r value of 5 mm because of the denser packaging of the smaller MCM−41 particles in comparison to the SBA−15 ones). These findings clearly confirmed that the use of GA-coupling and MSPs as the support provided high loading for all enzymes (just for information, the same remarkable results in terms of the amount of the immobilized enzyme, *ca.* 493 μg and 323 μg, were calculated for GOx-based mini-reactor (GOx−SBA15-$NH_{2\,(GA)}$) and Lac-based mini-reactor (Lac−MCM41-$NH_{2\,(GA)}$), respectively).

For comparison, the various classic biosensors (enzyme immobilized at the WE surface) are reported to contain the following quantities of, *e.g.*, AChE: 5.9 μg [138]; ChOx: 0.457 μg [139], 5.6 μg [140], 6.7 μg [138]; LOx: *ca.* 11.6 μg [141]; lactate dehydrogenase: 0.725 ± 0.08 μg [142] and 5.0 μg [143]; GOx: 2.6 μg [144], 6.53 μg [145]; Lac: 38.9 μg [146]; formaldehyde dehydrogenase *from Pseudomonas sp.: 2.6* μg [147], 92 μg [147].

However, it should be emphasized that all the above-calculated values refer to the total amount of immobilized enzymes, but not to their active fractions, which are expected to be lower [148]. In any case, even if 50 % of the immobilized enzyme in the prepared mini-reactor is inactive, the remaining amount of active enzyme will be still significantly larger than can be attached to the WE surface at all (research on the determination of the contents of active enzymes is currently being conducted, the results will be presented in further works).

3.3 Optimization of operating conditions of biosensors

To achieve the highest biosensor responses, key factors affecting both enzymatic and electrochemical reactions were evaluated. These included the pH and composition of the CS, the detection potential, the flow rate of the CS, and the injection volume. Figures illustrating the influence of the above parameters on the responses of each of the four developed biosensors are given in ***Publications I*** (Ch biosensor), ***II*** (ACh biosensor), ***III*** (UA biosensor), and ***VI*** (LA biosensor). A summary of the data, including the list of parameters, the ranges in which each variable was investigated (*in italics in brackets*), and the optimized values, is presented below in **Table 3.5**.

Composition of the CS and its pH. The activity of enzymes, which is determined by the protonated/deprotonated state of certain functional groups in the enzymatic active site, is considerably affected by the concentration of hydroxonium cations. In this regard, the pH of the solution is one of the most crucial factors in the efficient course of enzymatic transformations. Additionally, the electrochemical transduction also depends on the medium pH.

To avoid possible damage to the enzyme structure, which in turn would negatively affect its activity, the influence of the CS pH on each biosensor response was investigated in the pH range of activity of a particular enzyme (see **Table 3.5**). For this purpose, the CS with the composition of [0.1 mol L^{-1} PB, 1.0 mmol L^{-1} Na_2EDTA was used for Ch [**115**], ACh [**116**], and LA [**120**] biosensors, while three different CSs, namely [0.1 mol L^{-1} PB], [0.1 mol L^{-1} borate buffer (BB)], and [0.1 mol L^{-1} carbonate buffer (CB)] were utilized to cover the studied pH range (7.0 – 10.5) for UA biosensor [**117**]. In general, the dependences of the biosensor peak current on pH for four developed biosensors were typically bell-shaped. The maximum responses of Ch, ACh, UA, and LA biosensors were observed at pH values of 7.2, 8.0, 9.1, and 7.5, respectively, which were selected as optimal (these values differ from the optimal pH values for the free enzymes by 0.5 − 1.0).

Additionally, since the environment has a great influence on the enzyme catalytic activity, the different buffer solutions capable of providing the above-mentioned optimal pH values and their concentrations were compared. This investigation was performed for two biosensors, Ch and LA. First of all, [0.1 mol L^{-1} tris(hydroxymethyl)aminomethane (TRIS) buffer, 1.0 mmol L^{-1} Na_2EDTA, pH 7.2] and [0.1 mol L^{-1} PB, 1.0 mmol L^{-1} Na_2EDTA, pH 7.2] were compared for the Ch biosensor, while the comparison of [0.1 mol L^{-1} CB, pH 9.1] and

[0.1 mol L^{-1} BB, pH 9.1] was carried out for the UA biosensor. It was found that the Ch biosensor response was 2.0-fold higher using the CS with PB, which could be attributed to the higher electric conductivity (17.2 mS cm^{-1} and 4.51 mS cm^{-1} were measured for 0.1 mol L^{-1} PB and 0.1 mol L^{-1} TRIS buffer, respectively). For the UA biosensor, a 1.3-fold higher response was observed using the CS with BB. Next, for the Ch biosensor, PB solutions with different concentrations of 0.1, 0.2, and 0.5 mol L^{-1} were examined, whereas for the UA biosensor, 0.05 and 0.1 mol L^{-1} BB solutions were tested. As the concentration of buffers increased, the background current for both biosensors significantly increased, which is assumed because of the increased conductivity of the more concentrated buffer. For both biosensors, the highest peak current values were obtained at 0.1 mol L^{-1} buffer.

Finally, it should be noted that the Na_2EDTA in the CSs acted as a stabilizer for enzymes, slowing down and/or preventing their deactivation, and its adding was recommended by the manufacturer (Na_2EDTA was not used for the UA biosensor because it would deactivate the copper-containing UOx).

The detection potential (E_{det}) is a high-priority parameter for the amperometric measurements, which affects both the sensitivity and selectivity of the analysis. As seen from **Fig. 3.6**, in general, the dependence of the peak current on the shifting E_{det} to more negative values for all biosensors, regardless of the transducer type used (MF-AgSAE and TD-p-AgSA were tested for Ch [**115**], MF-AgSAE was used for ACh biosensor [**116**], TD-p-AgSA – for UA biosensor [**117**], and $AgA_{1.6}$-SPE – for LA biosensor [**120**]), includes the following three stages: a gradual increase, a plateau, and a signal deterioration (the latter was caused by the beginning of hydrogen release, that is, hydrogen microbubbles formed on the surface of the transducer reduced the WE surface area, which led to a decrease in the signal and deterioration of the repeatability of measurements).

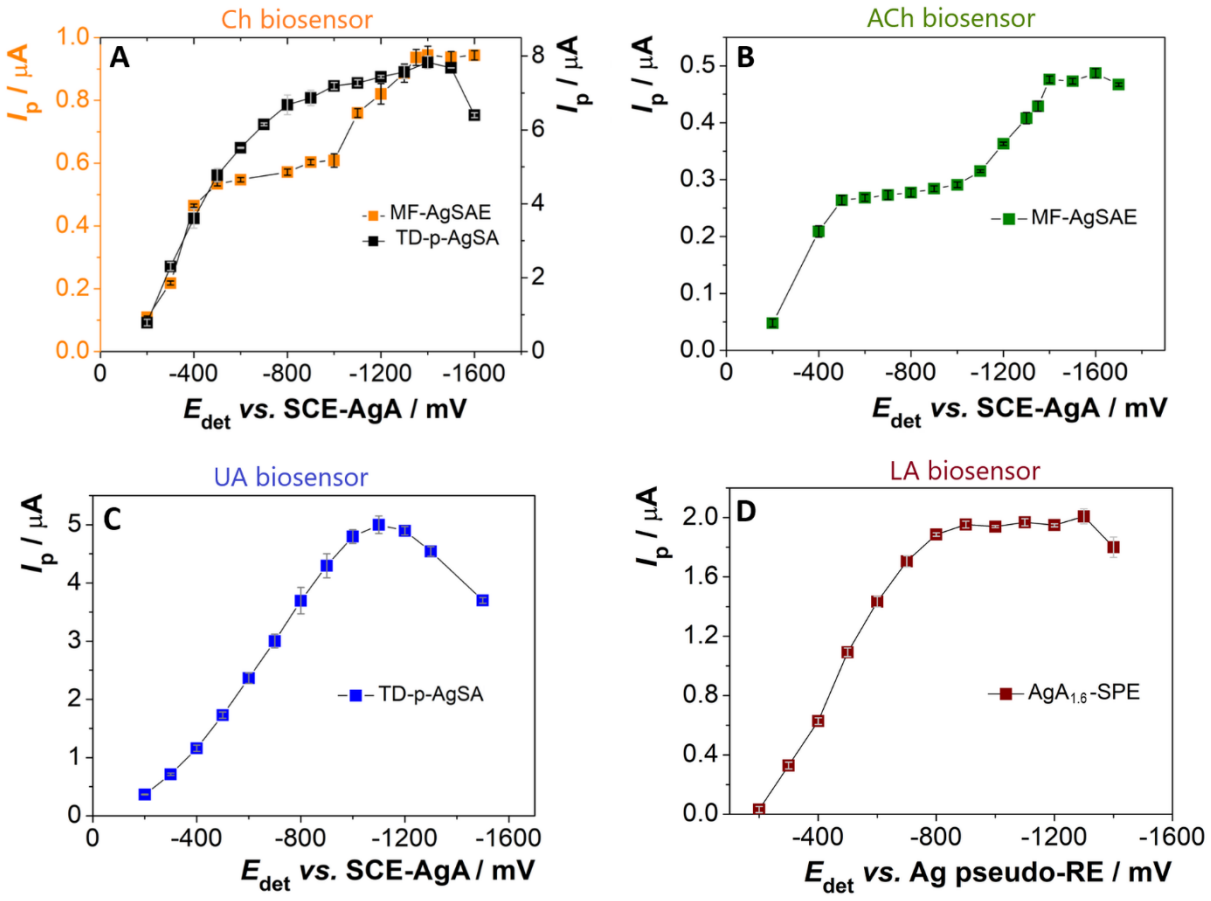

Fig. 3.6 Effect of the E_{det} on the response of the developed Ch (**A**), ACh (**B**), UA (**C**), and LA (**D**) biosensors containing different AgA-based transducers. The error bars correspond to the SD of five parallel measurements (n = 5). *Experimental conditions:* $c_{Ch} = c_{ACh} = c_{UA} = c_{LA}$ = 500 µmol L^{-1}; $V_{inj,\ Ch} = V_{inj,\ ACh} = V_{inj,\ UA} = V_{inj,\ LA}$ = 40 µL; v_{flow} of 0.2 (A, B, D) or 0.1 mL min^{-1} (C); CS: [0.1 mol L^{-1} PB, 1.0 mmol L^{-1} Na_2EDTA, pH 7.2] (A), [0.1 mol L^{-1} PB, 1.0 mmol L^{-1} Na_2EDTA, pH 8.0] (B), [0.1 mol L^{-1} BB, pH 9.1] (C), [0.1 mol L^{-1} PB, 1.0 mmol L^{-1} Na_2EDTA, pH 7.5] (D).

The E_{det} values at which these stages were observed differed for each of the developed biosensors because not only different types of transducers were utilized, but also the CSs with different pH values as well as different REs (the printed Ag pseudo-RE was employed for the LA biosensor, while the SCE-AgA was utilized for the other three biosensors). As expected, for all four biosensors, the highest responses were obtained at the highly negative E_{det} values, where the oxygen reduction involves a four-electron exchange (see **Fig. 3.6**).

Interestingly, the dependence obtained with MF-AgSAE, in contrast to those for two other detectors, TD-p-AgSA and $AgA_{1.6}$-SPE, clearly consisted of two well-separated waves, which well corresponds to the two two-electron stages of oxygen reduction. This behaviour is related to the type of MF-AgSAE surface, which is represented by liquid mercury (two well-separated

waves of oxygen reduction are similarly observed on hanging mercury drop electrode and dropping mercury electrode [76]).

Besides, in all cases, the baseline current of the recorded amperometric curves increased with the shift of E_{det} towards more negative values (*e.g.*, see *Appendices/**Publication VI**/Fig. 3(B) inset*). However, it had no negative influence on the sensitivity of the biosensors, because the signal-to-noise ratio did not deteriorate and the peak height was calculated by subtraction of the baseline current from the absolute peak current. Finally, the selected optimal E_{det} values for all biosensors are summarized in **Table 3.5**.

The flow rate of the CS (v_{flow}) plays an essential role for the biosensors in the FIA system because it primarily determines the contact time between enzyme and substrate, which directly affects the efficiency of the enzymatic conversion. This parameter also influences the course of the electrochemical reaction at the WE.

It was found that, despite the shortened time for the course of the enzymatic reactions, the signal of all four biosensors increased greatly (almost 2-fold) with an increase in v_{flow} from 0.05 to 0.2 mL min^{-1}. This tendency implies that each of the enzymatic reactions is adequately rapid, and here the substrate mass transport is the rate-determining step. With the exception of the Ch biosensor, where the response continued to enhance up to 0.4 mL min^{-1} (although not as sharply as before), further increases in v_{flow} (up to 0.25 mL min^{-1} for the ACh and UA biosensors or 0.35 mL min^{-1} for the LA biosensor) did not increase the peak height, as evidenced by the plateau. Obviously, the drop in the signals of UA and LA biosensors after 0.25 and 0.35 mL min^{-1}, respectively, was associated with the kinetic limitation of enzymatic reactions due to insufficient contact time between the substrate and the enzyme. Besides, as the v_{flow} increased, the following phenomena were observed, reflecting in the amperometric curves: (i) a decrease in the retention time and, as a result, the measurement time, (ii) a narrowing of the peak, (iii) an increase in the baseline current, and (iv) more noticeable oscillations produced by the pump. It is worth noting that the higher values, *i.e.*, $v_{flow} > 0.45$ mL min^{-1}, were not investigated, as the critical pressure in the FIA system was reached, leading to the loss of integrity between the capillary connections or the switching off of the syringe pump. For the ACh biosensor, the maximum studied value of v_{flow} was limited to 0.25 mL min^{-1} to avoid the leakage issue, as the critical pressure was already reached at the $v_{flow} \geq 0.3$ mL min^{-1}. This outcome was natural, as two mini-reactors integrated into a flow system caused a higher hydrodynamic resistance. Hence, the optimal values of the v_{flow}, summarized in **Table 3.5**, were selected as the most advantageous values taking into account the peak height and broadening, analysis time, and pressure in the flow system.

The injection volume (V_{inj}). The linear dynamic range (LDR) and the sensitivity of the biosensors in FIA may be manipulated by varying the substrate V_{inj}. In our case, the computer-controlled apparatus ensured the automatic filling of the injection loop with the necessary V_{inj}.

A remarkable improvement in the biosensor response was observed by increasing the V_{inj} up to 120 μL for Ch and ACh, 100 μL for UA, and 80 μL for LA biosensor (*e.g.*, a 3.2-fold signal increase was attained in the case of LA biosensor). This behaviour may be explained by the fact that during transportation, the zone of the substrate on both sides is significantly diluted by CS due to the notable difference between the v_{flow} of the CS in the centre of the capillary and near its walls. As the V_{inj} increased, the analyte zone expanded and the dilution effect became less influential, resulting in an enhanced biosensor response. Further increase in the V_{inj} up to 200 μL had no influence on the peak current, which remained almost unaltered for all biosensors due to the presence of the constant undiluted substrate zone. The choice of the optimal V values depends on the analysis requirements, considering sensitivity, the ability to register a well-defined and sharp peak, and last, but not least, measurement time. In view of this, the most favourable balance was considered to have been achieved at the values of 40 μL for the UA biosensor and 60 μL for the three others (see **Table 3.5**).

Finally, for the biosensor to work properly, it was necessary to provide **time for the enzymes to recover** (the reoxidation of the inactive reduced oxidase form by molecular oxygen; see ***subchapter 2.1***). The time required for the complete enzyme recovery in the mini-reactor avoiding its depletion was found to be about 160 s for UOx and 200 s for ChOx and LOx. Thus, considering the appropriate retention time, it was necessary to keep the time between two injections about 360 s for the UA biosensor and 300 s for the Ch, ACh, and LA biosensors. Otherwise, the biosensor signals gradually decreased, especially it was clearly noticed when the same enzymatic mini-reactor was continuously utilized throughout the whole day. Importantly, during this enzyme recovery time, the CS must pass through the enzymatic mini-reactor to supply it with dissolved molecular oxygen. Accordingly, based on the above-mentioned data, the sample throughput outcomes using the developed biosensors in the case of their continuous work are 10 − 12 measurements/hour. Nevertheless, it is worth emphasizing that there is no need to add time for enzyme regeneration, thereby increasing the measurement time if only a few measurements are planned. The large amounts of the immobilized enzymes in the prepared enzyme mini-reactors compensates for the lack of the enzyme in the active form at least up to around 30 measurements.

Table 3.5 Summary of the studied ranges of the optimized parameters and their selected optimal values for further measurements.

Biosensor	**Parameter**			
	Composition of CS and its pH	E_{det} **/ mV**	v_{flow} **/ mL min^{-1}**	V_{inj} **/ µL**
	Selected optimal value *(studied range)*			
Ch	[0.1 mol L^{-1} PB, 1.0 mmol L^{-1} Na_2EDTA, pH 7.2] *(5.6...9.5)*	−1400[(a)] *(−200...−1700)*	0.2 *(0.05...0.4)*	60 *(20...200)*
ACh	[0.1 mol L^{-1} PB, 1.0 mmol L^{-1} Na_2EDTA, pH 8.0] *(6.0...9.0)*	−1400[(a)] *(−200...−1700)*	0.2 *(0.05...0.25)*	60 *(20...200)*
UA	[0.1 mol L^{-1} BB, pH 9.1] *(7.0...10.5)*	−1100[(a)] *(−200...−1500)*	0.1 *(0.05...0.3)*	40 *(20...180)*
LA	[0.1 mol L^{-1} PB, 1.0 mmol L^{-1} Na_2ETDA, pH 7.5] *(5.5...8.5)*	−900[(b)] *(−200...−1400)*	0.2 *(0.05...0.45)*	60 *(20...200)*

[(a)] *vs.* SCE-AgA

[(b)] *vs.* Ag pseudo-RE

3.4 Analytical performance

Under the optimized conditions (listed in **Table 3.5**), the concentration dependences of each target analyte using the developed biosensors were measured and are depicted in **Fig. 3.7**. The attained figures of merit are summarized in **Table 3.6** along with the limit of detection (LOD) and limit of quantification (LOQ) values calculated as a 3-fold and a 10-fold, respectively, of the SD of the intercept, divided by the slope of the corresponding calibration plot.

The comparison of the two types of the AgA-based transducers for the Ch determination showed, as expected, the outperformance of MF-AgSAE over TD-p-AgSA in terms of the achieved LOD value. Specifically, MF-AgSAE manifested 1.7-times lower LOD value (see *Appendices/**Publication I**/Table 1*). This suggests that the four-electron oxygen reduction on the ideally smooth surface of MF-AgSAE is more favourable than on the relatively rough surface of TD-p-AgSA. However, the reliable and well-repeatable signals without the statistically significant change in the peak height for Ch were observed on both transducers even without any pre-treatment between the measurements. Nevertheless, from the technical point of view, it was more convenient to work with the TD-p-AgSA, which was incorporated in the flow-through cell, because it was less challenging to get rid of the air bubbles. In the flow-through cell, the air bubbles easily went through the TD-p-AgSA with the flow of the CS, while they frequently stuck between the MF-AgSAE and the inlet capillary in the wall-jet cell distorting the measurements. The only way to get rid of them was to “flick” the tubing near the cell to dislodge the bubbles.

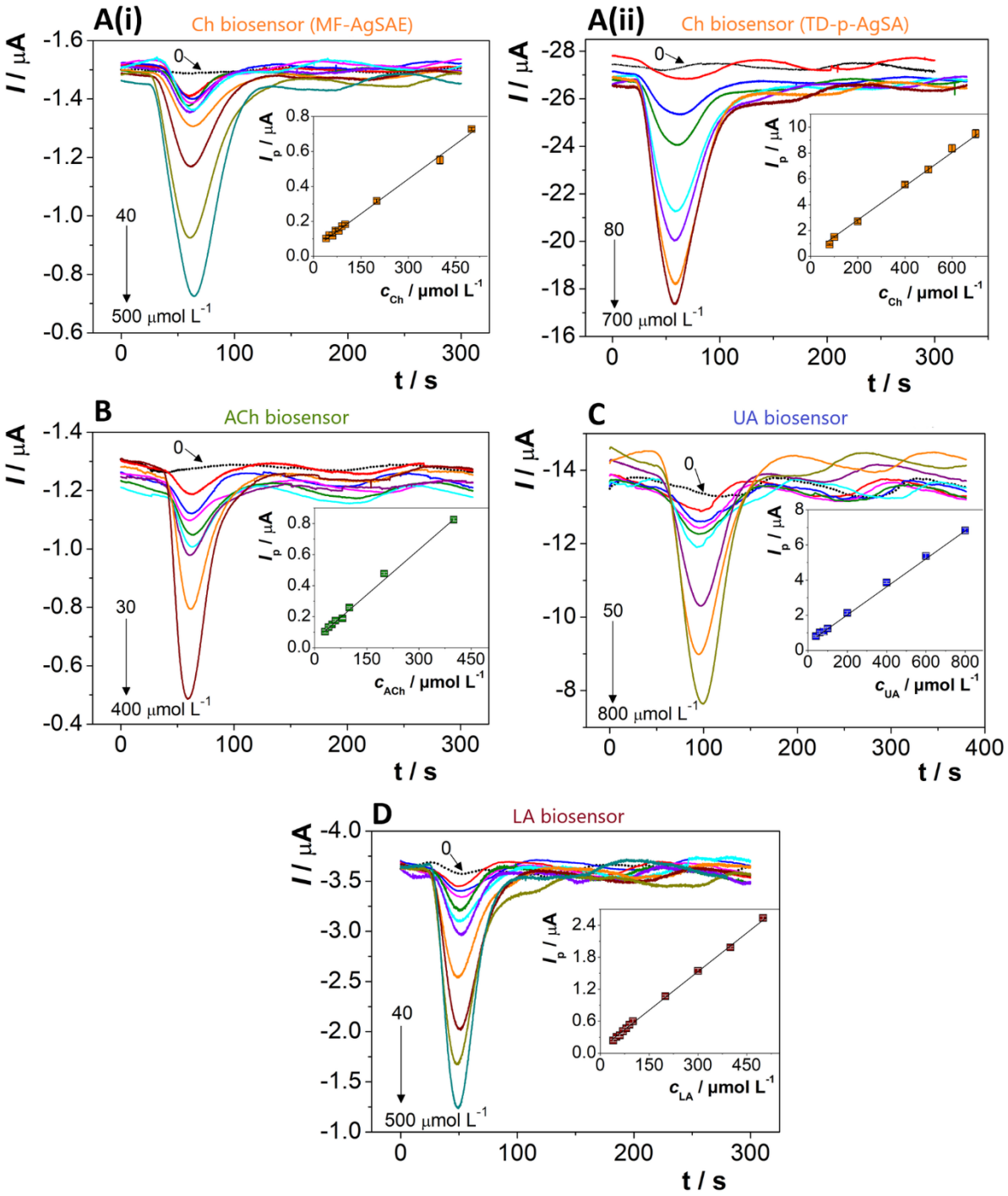

Fig. 3.7 Responses of the Ch (**A**) biosensors (using MF-AgSAE (**i**) or TD-p-AgSA (**ii**) as the transducer), ACh biosensor (**B**), UA biosensor (**C**), and LA biosensor (**D**), on the increasing concentration of the relevant substrate. Insets: corresponding calibration graphs. The measurement condition are listed in Table 3.5.

Table 3.6 Analytical figures of merit obtained for Ch, ACh, UA, and LA determination with the developed biosensors, with assessed LOD, LOQ, intra-day repeatability, and K_M^{app}.

Parameter	**Biosensor**				
	Ch[(a)]	**Ch**[(b)]	**ACh**[(c)]	**UA**[(d)]	**LA**[(e)]
LDR / μmol L^{-1}	40 − 500	80 − 700	30 − 400	50 − 800	40 − 500
Slope × 10^3 / μA L μmol^{-1}	1.32	137.4	1.97	8.03	4.7
SD of slope × 10^3 / μA L μmol^{-1}	0.026	0.237	0.053	0.147	0.082
Intercept × 10^3 / μA	48.03	273.8	53.09	510.5	84.7
SD of intercept × 10^3 / μA	5.84	10.263	8.89	56.	18.7
Correlation coefficient (R^2)	0.9965	0.9982	0.9949	0.9983	0.9970
LOD / μmol L^{-1}	13.0	22.0	13.6	18.5	12.0
LOQ / μmol L^{-1}	43.3	73.3	45.2	56.5	40.0
Intra-day repeatability [(f)] / %	3.1	4.5	2.8	2.8	1.7
K_M^{app} [(h)] / mmol L^{-1}	0.25	0.25	n.d.[(g)]	0.863	1.86

(a) ChOx−SBA15-$NH_{2\,(GA)}$ mini-reactor coupled to the MF-AgSAE
(b) ChOx−SBA15-$NH_{2\,(GA)}$ mini-reactor coupled to the TD-p-AgSA
(c) Two mini-reactors, AChE−SBA15-$NH_{2\,(GA)}$ and ChOx−SBA15-$NH_{2\,(GA)}$, coupled to the MF-AgSAE
(d) UOx(*B*)−MCM41-$NH_{2\,(GA)}$ mini-reactor coupled to the TD-p-AgSA
(e) LOx−SBA15-$NH_{2\,(GA)}$ mini-reactor coupled to the $AgA_{1.6}$-SPE
(f) Relative standard deviation for 11 successive measurements of 100 μmol L^{-1} Ch, 200 μmol L^{-1} ACh, 500 μmol L^{-1} UA, or 500 μmol L^{-1} LA standard solution
(g) Not determined
(h) Apparent Michaelis-Menten constant value

The analytical characteristics of the proposed biosensors were expected to be inferior to most biosensors proposed earlier (due to the dispersion of the analyte injection zone, FIA is generally characterized by worse sensitivity compared to batch analysis). A comparison of the analytical performance of the ACh and UA biosensors developed in this work with biosensors described in the literature in *Appendices/**Publication II**/Table 3* and *Appendices/**Publication III**/Table 3*, respectively.

Consequently, the achieved sensitivity is more than sufficient for the determination of UA and LA in the relevant samples (UA in urine, LA in the different biological fluids, wine, and dairy products). As for the Ch and ACh biosensors, the obtained sensitivity covers the concentration ranges of these compounds in pharmaceuticals and blood serum, but only for the healthy conditions. However, decreased levels of Ch and ACh in the case of, *e.g.*, Azheimer's disease (<10 μmol L^{-1}) are below the LOD value. Nevertheless, the developed biosensors can at least be considered useful as qualitative tools for distinguishing between healthy and abnormally low levels of Ch and ACh (if the concentrations of these compounds are not detectable, this automatically indicates a potential patient with the pathological decreased Ch or ACh content). However, future research should aim to improve sensitivity of the proposed biosensing platform.

In order to evaluate the reliability of the determination with the proposed biosensors, first of all, the intra-day repeatability of the eleven successive replicate measurements (n = 11) for 100 μmol L^{-1} Ch, 200 μmol L^{-1} ACh, 500 μmol L^{-1} UA, and 500 μmol L^{-1} LA solution was investigated. As shown in Table 3.6, the relative standard deviation (RSD) values for all biosensors were estimated to be < 5.0 %, demonstrating excellent repeatability of recorded peak currents, as well as no surface fouling of the AgA-based transducers between measurements. In addition, the repeatability of the mini-reactor preparation was evaluated. For this purpose, two representatives of each mini-reactor (three in the case of UOx(*B*)) were independently prepared. The RSD values of 4.7 % for Ch, 3.4 % for ACh, 3.9 % for UA, and 5.8 % for LA biosensors reflect the fact that the preparation of all enzyme-based mini-reactors using the GA technique has good repeatability. Furthermore, by statistically processing ten measurements for 500 μmol L^{-1} LA with two independently constructed $AgA_{1.6}$-SPEs (five measurements for each), the calculated 3.5% RSD reveals the good repeatability and reliability of the proposed electrochemical approach to the design of the amalgam SPEs.

Finally, the calculated apparent Michaelis-Menten constant (K_M^{app}) magnitudes for the Ch (0.25 mmol L^{-1}), UA (0.86 mmol L^{-1}), and LA (1.86 mmol L^{-1}) biosensors were comparable

or lower than the reported values by other researchers (for comparison see data in [**115-117**, **120**]). Such low K_M^{app} values indicate the high catalytic efficiency at low substrate concentrations, and thus the rapid kinetics of the enzymatic reactions.

Last, but not least, while offering sufficient analytical performance some other important advantages can be claimed for the biosensors described here against others. The most essential is the independence of the detection and biorecognition parts. Accordingly, one enzymatic mini-reactor can be easily and quickly replaced with another, allowing to start detection another analyte in several minutes. Moreover, the working electrode can be utilized for other purposes. Finally, the elaborated biosensors are simple and cost-effective in terms of design, and their operation in FIA ensures high sample throughput with the low consumption of the analyte. All these benefits point to the perspective application of the developed biosensors in the routine analysis.

3.5 Selectivity

Since AA, UA, and dopamine are electrochemically active substances, they are classified as the most common compounds that interfere in biosensing analysis with amperometric detection, and many previously reported electrochemical biosensors often suffer from varying degrees of interference [149-154]. In our case, the use of a negative E_{det} is of fundamental importance, as it avoids the common problems associated with the interference effect from electrooxidizable species. Therefore, to confirm the selectivity of the developed amperometric biosensors, the interference of electroactive substances, in particular AA, UA, dopamine, and urea, as well as glucose, which usually coexists in sample matrices with target analytes, was investigated. The study was performed at a concentration ratio of 10:1 target analyte/glucose (5:1 for LA biosensor) and 1:1 target analyte/other interferents (1:0.2 in the case of UA/AA). The results are summarized in **Fig.3.8**.

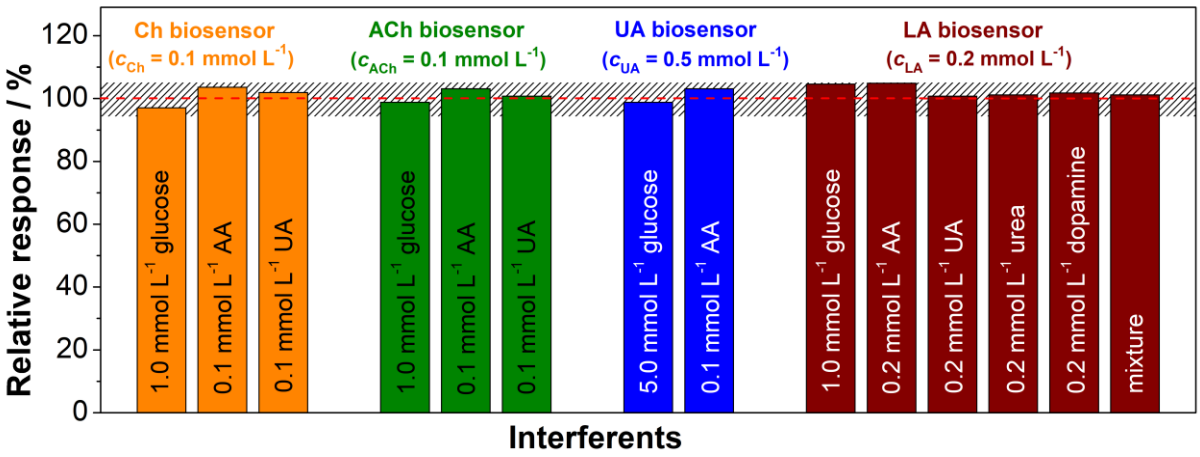

Fig. 3.8 Relative responses of the prepared Ch (orange bars), ACh (green bars), UA (blue bars), and LA (cherry bars) biosensors to the relevant substrates (100 µmol L^{-1} Ch, 100 µmol L^{-1} ACh, 500 µmol L^{-1} UA, and 200 µmol L^{-1} LA, respectively) obtained in the presence of the interfering compounds. The dashed area corresponds to a tolerated ± 5% alteration in the biosensor peak height. The dashed red line at 100 % represents the biosensor signals in the absence of any interferents.

As is evident in **Fig. 3.8**, none of the interfering compounds caused the biosensor signals to alter by more than the ± 5.0% tolerance limit. Moreover, when LA was mixed with all investigated agents, only a slight increase of 1.2 % was observed. These data clearly demonstrate that the tested possible interferences have a negligible effect on biosensor

responses, and thus the proposed biosensors are able to detect the target analytes in a selective manner.

In addition, the specificity of the developed ACh biosensor to an analogue structurally similar to AChE, namely succinylcholine, was investigated in order to find out whether this biosensor is suitable for monitoring the concentration of succinylcholine in pharmaceutical preparations (succinylcholine is a medication used to cause short-term paralysis as part of general anaesthesia [155]). This would allow expanding the field of the biosensor applications. It is worth noting that ACh and succinylcholine are not present together in the pharmaceuticals, since their functions are quite different. Recording the response of the biosensor containing AChE−SBA15-$NH_{2\ (GA)}$ and ChOx−SBA15-$NH_{2\ (GA)}$ mini-reactors to 500 μmol L^{-1} succinylcholine, no peak was observed. It reveals that AChE does not exhibit specificity to succinylcholine and, regrettably, the developed biosensor cannot be applied to monitor succinylcholine content in pharmaceuticals.

3.6 Operational and storage stability

First, investigating the operational stability of the Ch biosensor with the ChOx−SBA15-$NH_{2\ (GA)}$ mini-reactor, it was found that the biosensor response initially declined sharply during the first *ca.* 100 measurements, followed by a much slower, monotonic decrease over the next recorded *ca.* 600 measurements. For the ACh biosensor, the signal depended on the number of measurements in a similar way, *i.e.,* a decrease during the first approximately 100 uses, after which the response gradually dropped over the following *ca.* 300 measurements. The reason for such a rapid decrease at the beginning might arise from the leaching of the non-immobilized ChOx. Despite the presence of APTES and GA layers, the similar dimensions of the ChOx molecule (~4.6 nm × 7.0 nm × 8.8 nm [140]) with the SBA−15 pore (~ 7 nm) suggest that some amount of ChOx, in contrast to the larger AChE molecule (*ca.* 10 nm × 15 nm × 20 nm [138]) could partially penetrate the pores of SBA−15. Since this decrease was most likely not caused by the deactivation of the covalently immobilized enzyme, the results of the first 100 measurements were not reasonably taken into account when assessing the reusability of the Ch and ACh biosensors. It should be noted that this trend, a sharp decline in response after the first measurements, was not observed for the other two biosensors, for the determination of LA and UA, presumably due to the mismatch of the pore size of SBA−15 to accommodate LOx (*ca.* 8 nm assuming it is spherical [141]), as well as the pore size of MCM−41 (2.1 – 2.7 nm) for UOx(*B*). Therefore, it can be concluded that the Ch biosensor maintained 77.6 % of its performance after *ca*. 600 measurements (over 100 days), while, for the ACh biosensor, 79.6 % of the initial response remained after *ca.* 300 measurements (over 100 days). Although the response of both biosensors decreased, most likely due to the limited stability of ChOx, the achieved reusability is much superior to that of most of Ch (50 %/28 measurements [156], 50 %/100 uses [157], 50 %/255 measurements [158]) and ACh (50%/100 measurements [159], 83.1 %/18 uses [160]) biosensors reported before. Nevertheless, the biosensors could be successfully used further as the decreased stability does not influence the precision of the determination, but for evaluation, the methods of standard addition or comparison with the analyte standard solution should be applied.

The more impressive results were achieved with two other biosensors. It was found that the developed UA and LA biosensors demonstrate effective operational stability, as evidenced by no drop in peak current after 600 measurements (over 50 days) and 350 measurements (over 120 days), respectively. Besides, these data are only interim and research is ongoing. As most biosensors described in the literature can be commonly used for a lower measurement number

(UA: 90%/30 measurements [161], 90 %/120 measurements [162], 85 %/200 measurements [163]; LA: 88.3 %/18 measurements [164], 94%/60 measurements [143]), these results clearly indicate the extremely high operational stability of the constructed UA and LA biosensors, which is due to the high content of immobilized enzymes in the mini-reactors.

Next, the storage stability of the four developed biosensors, which is related to the individual shelf life of the immobilized enzymes under the storage conditions, was evaluated. All mini-reactors were stored at 4 °C immersed in a solution corresponding to the optimized CS for the respective biosensor (see **Table 3.5**). In practice, the current response of each developed biosensor to the corresponding 500 μmol L^{-1} analyte was measured regularly (approximately every 20 – 30 days) for 1 year and normalized to the initial value obtained on the first day, assumed to be 100 %. In addition, to verify the reliability of the results, for UOx(*B*) and LOx, two independently prepared mini-reactors were tested in parallel. All four biosensors were found to exhibit practically stable peaks, as their currents fluctuated throughout the test period but did not differ from the initial value by more than ±10 %. The important thing is that no progressive drop in biosensor signals was observed. These results indicate the exceptional storage stability, much better for the previously proposed biosensors (comparison data in *Appendices/**Publication II**/Tables 3* and *Appendices/**Publication III**/Tables 3* clearly demonstrate it). On the basis of this observation, it can be inferred that all enzymes, *i.e.,* ChOx, AChE, UOx, and LOx, covalently immobilized on the MSPs-NH_2 *via* GA do not lose their activity at least for 1 year when stored at 4 °C, which reveals a long shelf life of the enzymatic mini-reactors. Given the rather low storage stability of free enzyme solutions (ChOx loses 60% of its activity within 80 days when stored at 4 ºC [140]), it can be argued that GA creates a favourable microenvironment that preserves the active conformation of immobilized enzymes, slowing down or preventing the processes of their denaturation and/or aggregation.

Such excellent results in terms of operational and storage stability, which are better than those obtained for numerous biosensors reported earlier, are, undeniably, of great value for the practical implementation of the proposed biosensors as promising commercial devices, which would significantly reduce the cost of analysis. Furthermore, it should be emphasized that similar good outcomes were achieved for the biosensor with the GOx-based mini-reactor, which may indicate the functionality and prospects of the proposed concept in terms of its wide application for the fabrication of other highly stable and reusable oxidoreductase-based biosensors.

3.7 Practical application

To prove the practical applicability of the newly developed biosensors, each of them was applied to the determination of the target analyte in the relevant samples, as shown in Table 3.6, using either the multiple standard addition method or a method of comparison with the standard solution. The latter approach was used only for the Ch determination in the pharmaceuticals (Lipovitan® DUO – tablets for healthy liver function and Otic solution® − ear drops). The results obtained are summarized in **Table 3.6**. Amperograms related to the analysis of urine and four LA-containing different samples by the standard addition method (spiking with three successive additions) can be found in *Appendices/**Publication III**/Fig. 8* and *Appendices/**Publication VI**/Fig. 5,* respectively.

It should be mentioned that the pre-treatment of all studied samples did not require any complex manipulations, *i.e.,* previous separation steps. Detailed procedures for sample pre-treatment, which mainly included dilution to fall within the linear range of the proposed biosensors, except for saliva, which was only filtered, are described in ***Publications I*, *III*,** and ***VI*.** Since no peak was detected by analysing the human plasma on the ACh content, it was then spiked with the standard ACh solution to provide a total concentration of 60 μmol L^{-1} (prior to the analysis, the spiked human plasma was diluted in 10 times by [0.1 mol L^{-1} PB, 1.0 mmol L^{-1} Na_2EDTA, pH 8.0]).

By measuring any sample solution without the enzymatic mini-reactor (two mini-reactors for ACh biosensor), the straight baseline without neither up nor down peaks, true for all four developed biosensors, was registered. This behaviour reveals that the recorded downward peak when the enzymatic mini-reactor(s) is/are connected corresponds to the reduction of oxygen consumed as a result of the (cascade for ACh) enzymatic conversion(s). Moreover, although pharmaceutical Lipovitan® DUO contains some electroreducible substances, such as riboflavin and thiamine hydrochloride (detailed composition of the tablets is given in *Appendices/**Publication I**/section 3.5*), in the absence of the ChOx-based mini-reactor, no substantial variations in the current, which could be caused by the reduction of these compounds at the MF-AgSAE, were recorded either.

Table 3.6 Results of the application of the developed biosensors for the analysis of real samples containing the relevant target analyte. The found content is presented in units commonly used for a particular type of analyte and sample. Uncertainty represents the SDs for 7 (for Ch) and 3 (for UA and LA) replicate determinations.

Analyte	**Sample**	**Found**	**Declared**	
Ch	Lipovitan® DUO	254.0 ± 87 mg	255 mg (1 tablet)	
	Otic solution®	142.8 ± 2.3 mg	140 mg (1 g of solution)	
Analyte	**Sample**	**Found**	**Normal range (Ref.)**	
UA	Human urine #1	3.93 ± 0.035 mmol L^{-1}	< 4.4 mmol L^{-1}	([88])
	Human urine #2	2.98 ± 0.043 mmol L^{-1}		
LA	Human saliva	87.5 ± 2.4 µmol L^{-1}	< 200 µmol L^{-1}	([165])
	Wine	1.36 ± 0.031 g L^{-1}	< 3.0 g L^{-1}	([99])
	Yogurt	0.78 ± 0.007 % (*w*/*w*)	~ 0.9 % (*w*/*w*)	([166])
	Kefir	1.27 ± 0.028 % (*w*/*w*)	0.9 – 1.1 % (*w*/*w*)	([167])

As is apparent from **Table 3.6**, the amounts of Ch found in both pharmaceuticals are in good agreement with the contents provided by the manufacturers, which proves the effectiveness of the developed ChOx-based biosensor. Besides, Student's *t*-test was employed to determine whether there is a significant difference between the found and declared amounts. Since, for Lipovitan® DUO and Otic solution®, the calculated t_6 values (six degrees of freedom) of 0.30 and 3.22, respectively, are less than the critical value of 3.707 (probability (P) = 0.01, two-tailed test), the null hypothesis is retained: there is no evidence of systematic errors and any discrepancies between the found and declared amounts arise solely as a result of random variation. The results of UA and LA determination also appear to be relevant as the concentrations found employing the corresponding constructed biosensors correlate well with the concentration levels that should be in the investigated actual samples. The correctness and accuracy of the UA and LA quantification were confirmed by the performance of the recovery tests in urine and saliva, respectively (see **Table 3.7**), in which high recoveries ranging from 95.0 to 105.1 % were attained. The results of the *t*-test, in turn, showed no evidence of systematic error (P = 0.05, two-tailed test). Despite the high degree of complexity of the matrix, a good recovery result was also achieved when determining ACh in the spiked human plasma.

Table 3.7 Recovery studies for ACh, UA, and LA quantification in human plasma, urine, and saliva samples, respectively, using the constructed relevant biosensors. Uncertainty represents the SDs for 4 (for ACh) and 3 (for UA and LA) replicate determinations.

Sample Analyte	***c* added / µmol L^{-1}**	***c* found / µmol L^{-1}**	**Recovery / %**	***t*-test[(a)]**
Human plasma				
ACh	60.0	58.4 ± 1.4	97.3 ± 2.4	2.24
Human urine				
UA	100.0	104.5 ± 3.2	104.5 ± 3.2	2.44
	200.0	197.4 ± 2.1	98.7 ± 1.2	2.14
Human saliva				
LA	50.0	47.5 ± 3.6	95.0 ± 3.7	1.24
	100.0	103.0 ± 2.4	103.0 ± 2.4	2.17
	150.0	145.6 ± 2.7	97.1 ± 2.2	2.82
	200.0	208.5 ± 3.9	105.1 ± 1.5	3.77

(a) $t = |\text{(average } c \text{ found} - c \text{ added)}\sqrt{N} / SD|$

It is worth noting that no pre-treatment of the AgA transducers between the parallel measurements during analysis of real samples was performed because no electrode fouling, which is a great complication in the electroanalysis, was observed. Besides, it should be clarified that all research with the LA biosensor, including >700 measurements, was performed in this work with a single $AgA_{1.6}$-SPE, as no electrode fouling was observed.

Overall, all four proposed biosensors can successfully detect target analytes without complex sample pre-treatment, providing good selectivity even in complex matrices such as human biological fluids, *i.e.*, plasma, saliva, and urine. The absence of passivation of the transducers and, as a result, the unnecessary stage of their cleaning leads to a simplification of the determination procedure and a reduction of the total analysis time. All these facts demonstrate the possible applications of the proposed biosensors as promising commercial devices in clinical analysis, food, and/or pharmaceutical industries.

4 Conclusion

This Ph.D. thesis presents the use of a concept involving the spatial separation of the enzymatic and detection parts combined with the principle of detecting enzymatically consumed oxygen to develop reusable and interference-free flow-through electrochemical biosensors. Based on this approach, four amperometric biosensors consisting of the enzymatic mini-reactor(s) and the AgA-based transducer were successfully elaborated for the selective and reliable determination of Ch, ACh, UA, and LA in FIA.

Three different AgA-based transducers have been used, such as TD-p-AgSA, MF-AgSAE, and AgA-SPE, with the latter two being developed as part of this PhD thesis. In addition, a wall-jet cell for the MF-AgSAE was also constructed. In order to ensure a secure and effortless fixation of the MF-AgSAE, the inlet capillary was cut off at the angle of 30 º. The AgA-SPEs were fabricated using a reliable and highly reproducible procedure based on automated and computer-controlled electrochemical deposition of mercury at commercially available Ag-SPEs. It was demonstrated that the PHE as well as mechanical characteristics of the AgA-SPEs are strongly dependent on the amount of deposited mercury, and the most favourable results were achieved for AgA-SPEs with 50% (*w/w*) mercury content. Most importantly, the newly prepared AgA-SPEs showed significantly more negative PHE values compared to the original Ag-SPEs.

Overall, all three AgA-transducers were successfully used as the detector parts of the constructed (bi)enzymatic biosensors for amperometric monitoring oxygen consumption by its four-electron reduction at highly negative detection potentials. In contrast to the common approach of H_2O_2 detection, this made it possible to avoid the interference effect of electrooxidizable compounds, as evidenced by the results of the selectivity study.

The second part of this Ph.D. thesis was focused on the selection of the most suitable protocol for the preparation of the enzymatic mini-reactors. For this purpose, the comprehensive comparison study of the different covalent immobilization techniques was performed using the testing enzymes GOx and Lac. In general, three different crosslinking agents (GA, EDC/NHS, and DSS) and five different supports (MSPs: MCM−41 and SBA−15, cellulose, carbonaceous powders: Gr and GC) were investigated. In addition, three different aminoalkylsilanes were tested to prepare aminated MCM−41, and two approaches were investigated for functionalization of carbon powders with $-NH_2$ groups, namely diazonium salt chemistry and silanization. A strong influence of the immobilization protocol used on the

resulting biosensor performance was observed, demonstrating that any variable in the covalent attachment protocol plays an important role. As a result, considering all aspects, attachment protocol using GA and aminated MSPs prepared with APTES was identified as the most suitable and used to prepare all target mini-reactors based on ChOx, AChE, UOx*(B)*, or LOx. The content of immobilized enzyme was determined by the Bradford method and amounted to be 476 μg of ChOx, 955 μg of UOx*(B)*, and 270 μg of LOx in the mini-reactors, indicating their high enzymatic capacity.

The great advantage of the developed biosensors is their exceptionally high operational and storage stability. Accordingly, Ch and ACh biosensors maintained *ca.* 77.6% and 79.6% of their initial responses after *ca.* 600 and 300 measurements, respectively. The more remarkable results were attained for UA and LA biosensors, as no decreases in their signals were observed after 600 measurements (over 50 days), and 350 measurements (over 120 days), respectively. It should be emphasized that achieved operational stability are much higher than those commonly reported. Besides, all enzymatic mini-reactors exhibited the high storage stability, demonstrating the ability to be stored at 4 °C for at least 1 year. Such good results in terms of stability and storage will significantly reduce the cost of analysis. Other advantages of the developed biosensors are their simplicity of design and ease of use. Importantly, it should be noted that no fouling of the surfaces of the AgA-based transducers was observed.

The Ch, UA, and LA elaborated biosensors were successfully applied for the analysis of the relevant analyte-containing samples (Ch biosensor – two pharmaceuticals; UA biosensor – human urine; LA biosensor – human saliva, wine, and dairy products). The practical applicability of the ACh biosensor was verified by the determination of the ACh content in the spiked human plasma.

Overall, the proposed platform, based on the spatially segregated biorecognition part coupled with a principle of detecting oxygen consumption using the AgA-transducer, is perspective, since it allows solving the common biosensors' limitations related to low operational stability and interference effect from the electrooxidizable compounds. Therefore, it can be used for the development of amperometric biosensors with other oxidase enzymes. However, as can be seen from the evaluated LOD values for the four constructed biosensors, this biosensor platform is suitable for analytes if an LOD value of around 10 μmol L^{-1} is sufficient for their quantification.

5 References

[1] L.C. Clark, C. Lyons, Electrode systems for continuous monitoring in cardiovascular surgery, Ann. NY Acad. Sci. , 102 (1962) 29.

[2] P. Bollella, Enzyme-based amperometric biosensors: 60 years later … Quo Vadis?, Anal. Chim. Acta, 1234 (2022) 340517.

[3] P. Bollella, L. Gorton, Enzyme based amperometric biosensors, Curr. Opin. Electrohem., 10 (2018) 157-173.

[4] E.B. Bahadir, M.K. Sezginturk, Applications of commercial biosensors in clinical, food, environmental, and biothreat/biowarfare analyses, Anal. Biochem., 478 (2015) 107-120.

[5] C.I.L. Justino, T.A. Rocha-Santos, A.C. Duarte, Review of analytical figures of merit of sensors and biosensors in clinical applications, TrAC, Trends Anal. Chem., 29 (2010) 1172-1183.

[6] S.N. Topkaya, M. Azimzadeh, M. Ozsoz, Electrochemical biosensors for cancer biomarkers detection: recent advances and challenges, Electroanalysis, 28 (2016) 1402-1419.

[7] M.I. Prodromidis, M.I. Karayannis, Enzyme based amperometric biosensors for food nalysis, Electroanalysis, 14 (2002) 241-261.

[8] S.D. Wijayanti, L. Tsvik, D. Haltrich, Recent advances in electrochemical enzyme-based biosensors for food and beverage analysis, Foods, 12 (2023) 3355.

[9] E. Pourbasheer, Z. Azari, M.R. Ganjali, Recent advances in biosensors based nanostructure for pharmaceutical analysis, Curr. Anal. Chem., 15 (2019) 152-158.

[10] M. Kundu, P. Krishnan, R.K. Kotnala, G. Sumana, Recent developments in biosensors to combat agricultural challenges and their future prospects, Trends Food Sci. Technol., 88 (2019) 157-178.

[11] G. Maduraiveeran, W. Jin, Nanomaterials based electrochemical sensor and biosensor platforms for environmental applications, Trends Environ. Anal. Chem., 13 (2017) 1172-1183.

[12] N. Nikolaus, B. Strehlitz, Amperometric lactate biosensors and their application in (sports) medicine, for life quality and wellbeing, Microchim. Acta, 160 (2008) 15-55

[13] M. Mehrvar, M. Abdi, Recent developments, characteristics, and potential applications of electrochemical biosensors, Anal. Sci., 20 (2004) 1113-1126.

[14] U. Saxena, A.B. Das, Nanomaterials towards fabrication of cholesterol biosensors: Key roles and design approaches, Biosens. Bioelectron., 75 (2016) 196-205.

[15] S.V. Dzyadevych, V.N. Arkhypova, A.P. Soldatkin, A.V. Elskaya, C. Martelet, N. Jaffrezic-Renault, Amperometric enzyme biosensors: past, present and future, ITBM-RBM, 29 (2008) 171-180.

[16] I.S. Kucherenko, O.O. Soldatkin, S.V. Dzyadevych, A.P. Soldatkin, Electrochemical biosensors based on multienzyme systems: Main groups, advantages and limitations − A review, Anal. Chim. Acta, 1111 (2020) 114-131.

[17] I.S. Kucherenko, Y.V. Topolnikova, O.O. Soldatkin, Advances in the biosensors for lactate and pyruvate detection for medical applications: A review, Trends Anal. Chem., 2019 (2019) 160-172.

[18] C.S. Pundir, R. Devi, Biosensing methods for xanthine determination: A review, Enzyme Microb. Technol., 57 (2014) 55-62.

[19] G. Rocchitta, A. Spanu, S. Babudieri, G. Latte, G. Madeddu, G. Galleri, S. Nuvoli, P. Bagella, M.I. Demartis, V. Fiore, R. Manetti, P.A. Serra, Enzyme biosensors for biomedical applications: strategies for safeguarding analytical performances in biological fluids, Sensors, 16 (2016) 780.

[20] A.M. Azevedo, D.M.F. Prazeres, J.M.S. Cabral, L.P. Fonseca, Ethanol biosensors based on alcohol oxidase, Biosens. Bioelectron., 21 (2005) 235-247.

[21] J. Ahlawat, M. Sharma, C.S. Pundir, Advances in biosensor development for detection of acetylcholine, Microchim. J., 190 (2023) 108620.

[22] P. Kanyong, F.D. Krampa, Y. Aniweh, G.A. Awandare, Enzyme-based amperometric galactose biosensors: a review, Microchim. Acta, 184 (2017) 3663-3671.

[23] V.N. Narwal, R. Deswal, B. Batra, V. Kalra, R. Hooda, M. Sharma, J.S. Rana, Cholesterol biosensors: A review, Steroids, 143 (2019) 69-17.

[24] S. Arshi, M. Nozari-Asbemarz, E. Magner, Enzymatic bioreacors:an electrochemical perspective, Catalysts, 10 (2020) 1232.

[25] J.M. Bolivar, F. Lopez-Gallego, Characterization and evaluation of immobilized enzymes for applications in flow reactors, Curr. Opin. Green Sustain. Chem., 25 (2020) 100349.

[26] L. Tamborini, P. Fernandes, F. Paradisi, F. Moninari, Flow reactors as complementary tools for biocatalytic process intensification, Trends Biotehnol., 36 (2018) 73-88.

[27] K. Majer-Baranyi, N. Adanyi, M. Varadi, Investigation of a multienzyme based amperometric biosensor for determination of sucrose in fruit juices, Eur. Food Res. Technol., 228 (2008) 139-144.

[28] M. Thiruppathi, C.-Y. Tsai, T.-W. Wang, Y. Tsao, T.-H. Wu, J. A. Ho, Simple and cost-effective enzymatic detection of cholesterol using flow injection analysis, Anal. Sci., 36 (2020) 1119-1124.

[29] C. Hou, N. Gheczy, D. Messmer, K. Szymanska, J. Adamcik, R. Mezzenga, A.B. Jarzebski, P. Walde, Stable immobilization of enzymes in a macro- and mesoporous silica monolith, ACS Omega, 4 (2019) 7795-7806.

[30] M.I. Prodromidis, C.D. Stalikas, SM. Tzouwara-Karayanni, M.I. Karayannis, Determination of glycerol in alcoholic beverages using packed bed reactors with immobilized glycerol dehydrogenase and an amperometric FIA system, Talanta, 43 (1996) 27-33.

[31] M. Etienne, L. Zhang, N. Vila, A. Walcarius, Mesoporous materials-based electrochemical enzymatic biosensors, Electoanalysis, 27 (2015) 2028-2054.

[32] E. Magner, Immobilisation of enzymes on mesoporous silicate materials, Chem. Soc. Rev., 42 (2013) 6213-6222.

[33] R. Fopase, S. Paramasivam, P. Kale, B. Paramasivam, Strategies, challenges and opportunities of enzyme immobilization on porous silicon for biosensing applications, J. Environ. Chem. Eng., 8 (2020) 104266.

[34] C. Ispas, I. Sokolov, S. Andreescu, Enzyme-functionalized mesoporous silica for bioanalytical applications, Anal. Bioanal. Chem., 393 (2009) 543-554.

[35] P. Zucca, E. Sanjust, Inorganic materials as supports for covalent enzyme immobilization: methods and mechanisms, Molecules, 19 (2014) 14139-14194.

[36] M. R. F. Cerqueira, M. S. F. Santos, R. C. Matos, I. G. R. Gutz, L. Angnes, Use of poly(methyl methacrylate)/polyethyleneimine flow microreactors for enzyme immobilization, Microchem. J., 118 (2015) 231-237.

[37] Y. Wang, Y. Hasebe, Glucose oxidase-modified carbon-felt-reactor coupled with peroxidase-modified carbon-felt-detector for amperometric flow determination of glucose, Mater. Sci. Eng. C, 32 (2012) 432-439.

[38] L.M.C. Ferreira, E.T. Da Costa, C.L. Do Lago, A. Angnes, Miniaturized flow system based on enzyme modified PMMA microreactor for amperometric determination of glucose, Biosens. Bioelectron., 47 (2013) 539-544.

[39] F.C. Moraes, I. Cesarino, D. L. C. Golinelli, S. A. S. Machado, Enzymatic Solid-Phase Reactor Based on Silica Organofunctionalized with p-Phenylenediamine for Electrochemical Detection of Phenolic Compounds, Sensor Lett., 10 (2012) 1-8.

[40] L.R. Denaday, M.V. Miranda, R.M.T. Sanchez, J.M.L. Martinez, L.V.L. Lupano, V.C.D. Orto, Development and characterization of a polyampholyte-based reactor immobilizing soybean seed coat peroxidase for analytical applications in a flow system, Biochem. Eng. J., 58-59 (2011) 57-68.

[41] A. Vig, A. Igloi, N. Adanyi, G. Gyemant, C. Csutoras, A. Kiss, Development and characterization of a FIA system for selective assay of L-ascorbic acid in food samples, Bioprocess Biosyst. Eng., 33 (2010) 947-952.

[42] Y. Iida, T. Kikuchi, I. Satoh, Electrochemical enhancement for flow-amperometric biosensing with an oxidase column, Sens. Actuators B Chem., 91 (2003) 175-179.

[43] R. A. de Abreu Franchini, M. A. C. Matos, R. Colombara, R. C. Matos, Differential amperometric determination of hydrogen peroxide in honeys using flow-injection analysis with enzymatic reactor, Talanta, 75 (2008) 301-306.

[44] C. Saby, T.V. Nguyen, J.H.T. Luong, An electrochemical flow analysis system for putrescine using immobilized putrescine oxidase and horseradish peroxidase, Electroanalysis, 16 (2004) 260-267.

[45] P. He, J. Davies, G. Greenway, S.J. Haswell, Measurement of acetylcholinesterase inhibition using bienzymes immobilized monolith micro-reactor with integrated electrochemical detection, Anal. Chim. Acta, 659 (2010) 9-14.

[46] M. Yakovleva, O. Buzas, H. Matsumura, M. Samejima, K. Igarashi, P.-O. Larsson, L. Gorton, B. Danielsson, A novel combined thermometric and amperometric biosensor for lactose determination based on immobilised cellobiose dehydrogenase, Biosens. Bioelectron., 31 (2012) 251-256.

[47] K. Mohns, W. Kunnecke, Flow analysis with membrane separation and time based sampling for ethanol determination in beer and wine, Anal. Chim. Acta, 305 (1995) 241-247.

[48] S.J. Shin, H. Yamanaka, H. Endo, E. Watanabe, Development of an octopine biosensor and its application to the estimation of scallop freshness, Enzyme Microb. Technol., 23 (1998) 10-13.

[49] N. Sato, K. Usui, H. Okuma, Development of a bienzyme reactor sensor system for the determination of ornithine, Anal. Chim. Acta, 456 (2002) 219-226.

[50] M.-A. Carsol, M. Mascini, Development of a system with enzyme reactors for the determination of fish freshness, Talanta, 47 (1998) 335-342.

[51] H. Okuma, H. Takahashi, S. Yazawa, S. Sekimukai, Development of a system with double enzyme reactors for the determination of fish freshness, Anal. Chim. Acta, 260 (1992) 93-98.

[52] S.A.M. Marzouk, J.D. Haddow, A. Amin, Flow injection determination of sialic acid based on amperometric detection, Sens. Actuators B Chem., 157 (2011) 647-653.

[53] E. Salinas, V. Rivero, A.A.J. Torriero, D. Benuzzi, M.I. Sanz, J. Raba, Multienzymatic-rotating biosensor for total cholesterol determination in a FIA system, Talanta, (2006) 244-250.

[54] L. Novotny, B. Yosypchuk, Solid silver amalgam electrode, Chem. Listy, 94 (2000) 1118-1120.

[55] B. Yosypchuk, J. Barek, Analytical applications of solid and paste amalgam electrodes, Crit. Rev. Anal. Chem. , 39 (2009) 189-203.

[56] A. Danhel, J. Barek, Amalgam electrodes in organic electrochemistry, Curr. Org. Chem., 15 (2011) 2957-2969.

[57] J. Barek, F. Marques, The use of amalgam electrodes for monitoring of organic compounds: overview of papers published from 2011 to 2023, Monatsh. Chem., 154 (2023) 949-955.

[58] B. Yosypchuk, V. Marecek, Properties of thiolate monolayers formed on different amalgam electrodes, J. Electroanal. Chem., 653 (2011) 7-13.

[59] B. Josypčuk, M. Fojta, O. Yosypchuk, Thiolate monolayers formed on different amalgam electrodes. Part II: Properties and application, J. Electroanal. Chem., 694 (2013) 84-93.

[60] I. Jiranek , V. Cerveny , J. Barek, P. Rychlovsky, Comparison of mercury vapor pressure of silver amalgam-based electrode materials using AAS, Anal. Lett., 43 (2010) 1387-1399.

[61] D. Goncalves-Filho, C.C.G. Silva, D. De Souza, Pesticides determination in foods and natural waters using solid amalgam based electrodes: Challenges and trends, Talanta, 212 (2020) 120756.

[62] S. Smarzewska, R. Metelka, B. Bas, K. Vytras, Recent applications of silver amalgam electrodes for analysis of pharmaceuticals and vitamins, Curr. Med. Chem., 25 (2018) 4138-4151.

[63] Š. Skalová, J. Langmaier, J. Barek, V. Vyskočil, T. Navrátil, Doxorubicin determination using two novel voltammetric approaches: A comparative study, Electrochim. Acta, 330 (2020) 135180.

[64] L. Bandžuchová, R. Šelešovská, T. Navrátil, J. Chýlková, Silver Solid Amalgam Electrode as a Tool for Monitoring the Electrochemical Reduction of Hydroxocobalamin, Electroanalysis, 25 (2013) 213-222.

[65] S. Tvorynska, B. Josypčuk, J. Barek, L. Dubenska, Electrochemical behavior and sensitive methods of the voltammetric determination of food azo dyes amaranth and allura red AC on amalgam electrodes, Food Anal. Meth., 12 (2019) 409-421.

[66] P. Juskova, V. Ostatna, E. Palecek, F. Foret, Fabrication and characterization of solid mercury amalgam electrodes for protein analysis, Anal. Chem., 82 (2010) 2690-2695.

[67] R. Fadrna, K. Cahova-Kucharikova, L. Havran, B. Yosypchuk, M. Fojta, Use of polished and mercury film-modified silver solid amalgam electrodes in electrochemical analysis of DNA, Electroanalysis, 17 (2005) 452-459.

[68] V. Svitkova, K. Nemcekova, V. Vyskocil, Application of silver solid amalgam electrodes in electrochemical detection of DNA damage, Anal. Bioanal. Chem., 414 (2022) 5435-5444.

[69] D. Hynek, J. Prasek, P. Koudelka, J. Chomoucka, L. Trnkova, V. Adam, J. Hubanek, R. Kizek, Advantages and progress in the analysis of DNA by using mercury an amalgam electrodes - review, Curr. Phys. Chem., 1 (2011) 299-324.

[70] A. Danhel, K.K. Shiu, B. Yosypchuk, J. Barek, K. Peckova, V. Vyskocil, The use of silver solid amalgam working electrode for determination of nitrophenols by HPLC with electrochemical detection, Electroanalysis, 21 (2009) 303-308.

[71] I. Jiranek, K. Peckova, Z. Kralova, J.C. Moreira, J. Barek, The use of silver solid amalgam electrode for voltammetric and amperometric determination of nitroquinolines, Electrochim. Acta, 54 (2009) 1939-1947.

[72] O. Yosypchuk, J. Karasek, V. Vyskocil, J. Barek, K. Peckova, The use of silver solid amalgam electrodes for voltammetric and amperometric determination of nitrated polyaromatic compounds used as markers of incomplete combustion, Sci. World J., 2012, Article ID 231986 (2012) 1-12.

[73] K. Peckova, L. Vrzalova, V. Bencko, J. Barek, Voltammetric and amperometric determination of N-nitroso antineoplastic drugs at mercury and amalgam electrodes, Collect. Czech. Chem. Commun., 74 (2009) 1697-1713.

[74] O. Josypčuk, Electrochemical biosensors and detectors based on silver solid amalgam for analysis in flow systems, in: Ph.D. thesis, Charles University in Prague, 2014, pp. 116.

[75] O. Josupčuk, J. Barek, B. Josypčuk, Application of non-stop-flow differential pulse voltammetry at a tubular detector of silver solid amalgam for electrochemical determination of lomustine (CCNU), Elctroanalysis, 26 (2014) 306-311.

[76] I.M. Kolthoff, C.S. Miller, The reduction of oxygen at the dropping mercury electrode, J. Am. Chem. Soc., 63 (1941) 1013-1017.

[77] B. Josypčuk, J. Barek, O. Josypčuk, Flow electrochemical biosensors based on enzymatic porous reactor and tubular detector of silver solid amalgam, Anal. Chim. Acta, 778 (2013) 24-30.

[78] S.H. Zeisel, K.-A. Da Costa, Choline: an essential nutrient for public health, Nutr. Rev., 67 (2009) 615-623.

[79] Y.O. Ilcol, R. Ozbek, E. Hamurtekin, I.H. Ulus, Choline status in newborns, infants, children, breast-feeding women, breast-fed infants and human breast milk, J. Nutr. Biochem., 16 (2005).

[80] M.D. Spencer, T.J. Hamp, R.W. Reid, L.M. Fischer, S.H. Zeisel, A.A. Fodor, Association between composition of the human gastrointestinal microbiome and development of fatty liver with choline deficiency, Gastroenterology, 140 (2011) 976-986.

[81] H.M. Awwad, J. Geisel, R. Obeid, The role of choline in prostate cancer, Clin Biochem., 45 (2012) 1548-1553.

[82] E.L. Richman, S.A. Kenfield, M.J. Stampfer, E.L. Giovannucci, S.H. Zeisel, W.C. Willett, J.M. Chan, Choline intake and risk of lethal prostate cancer: Incidence and survival, Am. J. Clin. Nutr., 96 (2012) 855-863.

[83] M.E. Hasselmo, The role of acetylcholine in learning and memory, Curr. Opin. Neurobiol., 16 (2006) 710-715.

[84] N.I. Bohnen, R.L. Albin, The cholinergic system and Parkinson disease, Behav. Brain Res., 221 (2011) 564-573.

[85] S. Lombardo, U. Maskos, Role of the nicotinic acetylcholine receptor in Alzheimer's disease pathology and treatment, Neuropharmacology, 96 B (2015) 255-262.

[86] R. Sangubotla, J. Kim, Recent trends in analytical approaches for detecting neurotransmitters in Alzheimer's disease, Trends Anal. Chem., 105 (2018) 240-250.

[87] Y.S. Mineur, M.R. Picciotto, The role of acetylcholine in negative encoding bias: Too much of a good thing?, Eur. J. Neurosci., 53 (2021) 114-125.

[88] P. E. Erden, E. Kilic, A review of enzymatic uric acid biosensors based on amperometric detection, Talanta, 107 (2013) 312-323.

[89] F. Perez-Ruiz, N. Dalbeth, T.A. Bardin, A review of uric acid, crystal deposition disease, and gout, Adv. Ther., 32 (2015) 31-41.

[90] A. Dehghan, M. Van Hoek, E.J. Sijbrands, A. Hofman, J.C. Witteman, High serum uric acid as a novel risk factor for type 2 diabetes, Diabetes care, 31 (2008) 361-362.

[91] G. Lippi, M. Montagnana, M. Franchini, E.J. Favaloro, G. Targher, The paradoxical relationship between serum uric acid and cardiovascular disease, Clin. Chim. Acta, 392 (2008) 1-7.

[92] S. Bell, I. Kolobova, L. Crapper, C. Etnst, Lesch-Nyhan syndrome: models, theories, and therapies, Mol. Syndromol., 7 (2016) 302-311.

[93] M. Rentzos, C. Nikolaou, M. Anagnostouli, A. Rombos, K. Tsakanikas, M. Economou, A. Dimitrakopoulos, M. Karouli, D. Vassilopoulos, Serum uric acid and multiple sclerosis, Clin. Neurol. Neurosurg., 108 (2006) 527-531.

[94] O. Kruse, N. Grunnet, C. Barfod, Blood lactate as a predictor for in-hospital mortality in patients admitted acutely to hospital: a systematic review,, Scand. J. Trauma. Resusc. Emerg. Med., 19 (2011) 74.

[95] Z. Zhang, X. Xu, Lactate clearance is a useful biomarker for the prediction of all-cause mortality in critically ill patients, Crit. Care Med., 42 (2014) 2118-2125.

[96] K. Cox, M.N. Cocchi, J.D. Salciccioli, E. Carney, M. Howell, M.W. Donnino, Prevalence and significance of lactic acidosis in diabetic ketoacidosis, J. Crit. Care, 27 (2012) 132-137.

[97] F. Hirschhaeuser, U.G.A. Sattler, W. Mueller-Klieser, Lactate: A metabolic key player in cancer, Cancer Res., 71 (2011) 6921-6925.

[98] L. Rassaei, W. Olthuis, S. Tsujimura, E.J.R. Sudholter, A. van den Berg, Lactate biosensors: current status and outlook, Anal. Bioanal. Chim., 406 (2014) 123-137.

[99] J. Vicente, Y. Baran, E. Navascues, A. Santos, F. Calderon, D. Marquina, D. Rauhut, S. Benito, Biological management of acidity in wine industry: A review, Int. J. Food Microbiol., 375 (2022) 109726.

[100] Q. Wang, X. Wen, J. Kong, Recent progress on uric acid detection: a review, Crit. Rev. Anal. Chem., 50 (2020) 359-375.

[101] M.M. Phillips, Analytical approaches to determination of total choline in foods and dietary supplements, Anal. Bioanal. Chem., 403 (2012) 2103-2112.

[102] C.S. Pundir, V. Narwal, B. Batra, Determination of lactic acid with special emphasis on biosensing methods: A review, Biosens. Bioelectron., 86 (2016) 777-790.

[103] T.-H. Tsai, Separation methods used in the determination of choline and acetylcholine, J. Chromatogr. B, Biomed. Sci. Appl., 747 (2000) 111-122.

[104] S. Aafria, P. Kumari, S. Sharma, S. Yadav, B. Batra, J.S. Rana, M. Sharma, Electrochemical biosensing of uric acid: A review, Microchem. J., 182 (2022) 107945.

[105] M.F.M. Shakhih, A.S. Rosslan, A.M. Noor, S. Ramanathan, A.M. Lazim, A.A. Wahab, Enzymatic and non-enzymatic electrochemical sensor for lactate detection in human biofluids, J. Electrochem. Soc., 168 (2021) 067502.

[106] K. Rathee, V. Dhull, R. Dhull, S. Singh, Biosensors based on electrochemical lactate detection: A comprehensive review, Biochem. Biophys. Rep., 5 (2016) 35-54.

[107] P. Rahimi, Y. Joseph, Enzyme-based biosensors for choline analysis: A review, Trends Anal. Chem., 110 (2019) 367-374.

[108] S. Pati, M. Quinto, F. Palmisano, Flow injection determination of choline in milk hydrolysates by an immobilized enzyme reactor coupled to a selective hydrogen peroxide amperometric sensor, Anal. Chim. Acta, 594 (2007) 234-239.

[109] P.C. Pandey, S. Upadhyay, H.C. Pathak, C.M.D. Pandey, I. Tiwari, Acetylthiocholine/acetylcholine and thiocholine/choline electrochemical biosensors/sensors based on an organically modified sol–gel glass enzyme reactor and graphite paste electrode, Sens. Actuators. B, 62 (2000) 109-116.

[110] Y. Lin, P. Yu, L. Mao, A multi-enzyme microreactor-based online electrochemical system for selective and continuous monitoring of acetylcholine, Analyst, 140 (2015) 3781-3787.

[111] Y. Wang, Y. Hasebe, Uricase-adsorbed carbon-felt reactor coupled with a peroxidase-modified carbon-felt-based H_2O_2 detector for highly sensitive amperometric flow determination of uric acid, J. Pharm. Biomed. Anal., 57 (2012) 125-132.

[112] S.A.M. Marzouk, H.E.M. Sayour, A.M. Ragab, W.E. Cascio, S.S.M. Hassan, Simple FIA-system for simultaneous measurements of glucose and lactate with amperometric detection, Electoanalysis, 12 (2000) 1304-1311.

[113] Z. Bori, G. Csifféry, D. Virág, M. Tóth-Markus, A. Kiss, N. Adányi, Determination of L-lactic acid content in foods by enzyme-based amperometric bioreactor, Electoanalysis, 24 (2012) 158-164.

[114] A.A.J. Torriero, E. Salinas, R. Battaglini, J. Raba, Milk lactate determination with a rotating bioreactor based on an electron transfer mediated by osmium complexes incorporating a continuous-flow/stopped-flow system, Anal. Chim. Acta, 498 (2003) 155-163.

[115] S. Tvorynska, J. Barek, B. Josypčuk, Amperometric biosensor based on enzymatic reactor for choline determination in flow systems, Electroanalysis, 31 (2019) 1901-1912.

[116] S. Tvorynska, J. Barek, B. Josypčuk, Acetylcholinesterase-choline oxidase-based mini-reactors coupled with silver solid amalgam electrode for amperometric detection of acetylcholine in flow injection analysis, J. Electroanal. Chem., 860 (2020) 113883.

[117] S. Tvorynska, J. Barek, B. Josypčuk, Flow amperometric uric acid biosensors based on different enzymatic mini-reactors: A comparative study of uricase immobilization, Sens. Actuators: B Chem., 344 (2021) 130252.

[118] B. Josypčuk, J. Langmaier, S. Tvorynska, Screen-printed amalgam electrodes, Sens. Actuators: B Chem., 347 (2021) 130583.

[119] S. Tvorynska, J. Barek, B. Josypcuk, Influence of different covalent immobilization protocols on electroanalytical performance of laccase-based biosensors, Bioelectrochemistry, 148 (2022) 108223.

[120] S. Tvorynska, J. Barek, B. Josypčuk, High-performance amperometric biosensor for flow injection analysis consisting of a replaceable lactate oxidase-based mini-reactor and a silver amalgam screen-printed electrode, Electrochim. Acta, 445 (2023) 142033.

[121] K. Novakova, V. Hrdlicka, T. Navratil, M. Harvila, J. Zima, J. Barek, Application of silver solid amalgam electrode for determination of formamidine amitraz, Monatsh. Chem., 147 (2016) 181-189.

[122] R. Selesovska, L. Bandzuchova, T. Navratil, J. Chylkova, Voltammetric determination of leucovorin using silver solid amalgam electrode, Electrochim. Acta, 60 (2012) 375-383.

[123] V. Hrdlicka, M. Choinska, B.R. Redondo, J. Barek, T. Navratil, Determination of heavy metal poisoning antidote 2,3-dimercapto-1-propanesulfonic acid using silver solid amalgam electrode, Electrochim. Acta, 354 (2020) 136623.

[124] B. Yosypchuk, M. Fojta, J. Barek, Preparation and properties of mercury film electrodes on solid amalgam surface, Electroanalysis, 22 (2010) 1967-1973.

[125] A.J. Bard, L.R. Faulkner, Electrochemical methods: fundamentals and applications, John Wiley and Sons, New York, 2001.

[126] A.G.-M. Ferrari, C.W. Foster, P.J. Kelly, D.A.C. Brownson, C.E. Banks, Determination of the electrochemical area of screen-printed electrochemical sensing platforms, Biosensors, 8 (2018) 1-10.

[127] A. Sassolas, L.J. Blum, B.D. Leca-Bouvier, Immobilization strategies to develop enzymatic biosensors, Biotechnol. Adv., 30 (2012) 489-511.

[128] S. Tvorynska, J. Barek, B. Josypčuk, A comparative study of covalent glucose oxidase and laccase immobilization techniques at powdered supports for biosensors fabrication, in: In: 16th International Students Conference “Modern Analytical Chemistry”. Prague, Czech Republic, 2020, pp. 25-30.

[129] D.I. Bezbradica, C. Mateo, J.M. Guisan, Novel support for enzyme immobilization prepared by chemical activation with cysteine and glutaraldehyde, J. Mol. Catal. B Enzym., 102 (2014) 218-224.

[130] G.T. Hermanson, Bioconjugate techniques. 2nd ed, Academic Press, San Diego, USA, 2008.

[131] I. Migneault, C. Dartiguenave, M.J. Bertrand, K.C. Waldron, Glutaraldehyde: behavior in aqueous solution, reaction with proteins, and application to enzyme crosslinking, BioTechniques, 37 (2004) 790-802.

[132] D.-M. Liu, C. Dong, Recent advances in nano-carrier immobilized enzymes and their applications, Process Biochem., 92 (2020) 464-475.

[133] Y. Gao, I. Kyratzis, Covalent immobilization of proteins on carbon nanotubes using the cross-linker 1-ethyl-3-(3-dimethylaminopropyl)carbodiimide - A critical assessment, Bioconjug. Chem., 19 (2008) 1945-1950.

[134] M.M. Bradford, Rapid and sensitive method for the quantitation of microgram quantities of protein utilizing the principle of protein-dye binding, Anal Biochem, 72 (1976) 248-254.

[135] L.F. Bautista, G. Moralez, R. Sanz, Immobilization strategies for laccase from Trametes versicolor on mesostructured silica materials and the application to the degradation of naphthalene, Bioresour Technol, 101 (2010) 8541-8548.

[136] P.C. Gunaratna, G.S. Wilson, Optimization of multienzyme flow reactors for determination of acetylcholine, Anal. Chem., 62 (1990) 402-407.

[137] C. Tamm, Pig liver esterase catalyzed hydrolysis: Substrate specificity and stereoselectivity, Pure Appl Chem., 64 (2009) 1187-1191.

[138] T. Shimomura, T. Itoh, T. Sumiya, F. Mizukami, M. Ono, Amperometric biosensor based on enzymes immobilized in hybrid mesoporous membranes for the determination of acetylcholine, Enzyme Microb. Technol., 45 (2009) 443-448.

[139] Md.A. Rahman, D.-S. Park, Y.-B. Shim, A performance comparison of choline biosensors: anodic or cathodic detections of H_2O_2 generated by enzyme immobilized on a conducting polymer, Biosens. Bioelectron., 19 (2004) 1565-1571.

[140] T. Shimomura, T. Itoh, T. Sumiya, F. Mizukami, M. Ono, Amperometric determination of choline with enzyme immobilized in a hybrid mesoporous membrane, Talanta, 78 (2009) 217-220.

[141] T. Shimomura, T. Sumiya, M. Ono, T. Ito, T. Hanaoka, Amperometric l-lactate biosensor based on screen-printed carbon electrode containing cobalt phthalocyanine, coated with lactate oxidase-mesoporous silica conjugate layer, Anal. Chim. Acta, 714 (2012) 114-120.

[142] M.M. Rahman, M.J.A. Shiddiky, Md.A. Rahman, Y.-B. Shim, A lactate biosensor based on lactate dehydrogenase/nictotinamide adenine dinucleotide (oxidized form) immobilized on a conducting polymer/multiwall carbon nanotube composite film, Anal. Biochem., 384 (2009) 159-165.

[143] A.C. Pereira, M.R. Aguiar, A. Kisner, D.V. Macedo, L.T. Kubota, Amperometric biosensor for lactate based on lactate dehydrogenase and Meldola Blue coimmobilized on multi-wall carbon-nanotube, Sens. Actuators B Chem., 124 (2007) 269-276.

[144] M.F. Abasiyanik, M. Senel, Immobilization of glucose oxidase on reagentless ferrocene-containing polythiophene derivative and its glucose sensing application, J. Electroanal. Chem., 639 (2010) 21-26.

[145] H.B. Yildiz, S. Kiralp, L. Toppare, Y. Yagci, Immobilization of glucose oxidase in conducting graft copolymers and determination of glucose amount in orange juices with enzyme electrodes, Int. J. Biol. Macromol., 37 (2005) 174-178.

[146] T. Shimomura, T. Itoh, T. Sumiya, T. Hanaoka, F. Mizukami, M. Ono, Amperometric detection of phenolic compounds with enzyme immobilized in mesoporous silica prepared by electrophoretic deposition, Sens. Actuators B Chem., 1536 (2011) 361-368.

[147] T. Shimomura, T. Itoh, T. Sumiya, F. Mizukami, M. Ono, Electrochemical biosensor for the detection of formaldehyde based on enzyme immobilization in mesoporous silica materials, Sens. Actuators B Chem., 135 (2008) 268-275.

[148] P. Saengdee, W. Chaisriratanakul, W. Bunjongpru, W. Sripumkhai, A. Srisuwan, W. Jeamsaksiri, C. Hruanun, A. Poyai, C. Promptmas, Surface modification of silicon dioxide, silicon nitride and titanium oxynitride fo rlactate dehydrogenase immobilization, Biosens. Bioelectron., 67 (2015) 134-138.

[149] P. Gimenez-Gomez, M. Gutierrez-Capitan, F. Capdevila, A. Puig-Pujol, C. Fernandez-Sanchez, C. Jimenez-Jorquera, Monitoring of malolactic fermentation in wine using an electrochemical bienzymatic biosensor for L-lactate with long term stability, Anal. Chim. Acta, 905 (2016) 126-133.

[150] D. Chan, M.M. Barsan, Y. Korpan, C.M.A. Brett, L-lactate selective impedimetric bienzymatic biosensor based on lactate dehydrogenase and pyruvate oxidase, Electrochim. Acta, 231 (2017) 209-215.

[151] A.T. Tunc, E. Aynaci Koyuncu, F. Arslan, Development of an acetylcholinesterase–choline oxidase based biosensor for acetylcholine determination, Artif. Cells Nanomed. Biotechnol., 44 (2016) 1659-1664.

[152] A. Guerrieri, V. Lattanzio, F. Palmisano, P.G. Zambonin, Electrosynthesized poly(pyrrole)/poly(2-naphthol) bilayer membrane as an effective anti-interference layer for simultaneous determination of acethylcholine and choline by a dual, Biosens. Bioelectron., 21 (2006) 1710-1718.

[153] C. Cheng, C.-Y. Kao, An electrochemical biosensor with uricase immobilized on functionalized gold coated copper wire electrode for urinary uric acid assay, Electroanalysis, 28 (2016) 695-703.

[154] F. Zhang, C. Li, X. Li, X. Wang, Q. Wan, Y. Xian, L. Jin, K. Yamamoto, ZnS quantum dots derived a reagentless uric acid biosensor, Talanta, 68 (2006) 1353-1358.

[155] L. Huang, C.N. Sang, M.S. Desai, A Chronology for the Identification and disclosure of adverse effects of succinylcholine, J. Anesth. Hist., 5 (2019) 65-84.

[156] T. Ouiram, C. Moonla, A. Preechaworapun, S. Muangpil, W. Maneeprakorn, T. Tangkuaram, Choline oxidase based composite ZrO_2@AuNPs with Cu_2O@MnO_2 platform for signal enhancing the choline biosensors, Electroanalysis, 33 (2021) 455-463.

[157] S. Pundir, N. Chauhan, J. Narang, C.S. Pundir, Amperometric choline biosensor based on multiwalled carbon nanotubes/zirconium oxide nanoparticles electrodeposited on glassy carbon electrode, Anal. Biochem., 427 (2012).

[158] S. Sen, A. Gulce, H. Gulce, Polyvinylferrocenium modified Pt electrode for the design of amperometric choline and acetylcholine enzyme electrodes, Biosens. Bioelectron., 19 (2004) 1261-1268.

[159] N. Chauhan, C.S. Pundir, Amperometric determination of acetylcholine – A neurotransmitter, by chitosan/gold-coated ferric oxide nanoparticles modified gold electrode, Biosens. Bioelectron., 61 (2014) 1-8.

[160] E. Aynaci, A. Yasar, F. Arslan, An amperometric biosensor for acetylcholine determination prepared from acetylcholinesterase-choline oxidase immobilized in polypyrrole-polyvinylsulpfonate film, Sens. Actuators B Chem., 202 (2014) 1028-1036.

[161] K. Arora, G. Sumana, V. Saxena, R.K. Gupta, S.K. Gupta, J.V. Yakhmi, M.K. Pandey, S. Chand, B.D. Malhorta, Improved performance of polyaniline-uricase biosensor, Anal. Chim. Acta, 594 (2007) 17-23.

[162] R. Devi, C. S. Pundir, Construction and application of an amperometric uric acid biosensor based on covalent immobilization of uricase on iron oxide nanoparticles/chitosan-g-polyaniline composite film electrodeposited on Pt electrode, Sens. Actuators B, 193 (2014) 608-615.

[163] N. Chauhan, A. Kumar, C.S. Pundir, Construction of an uricase nanoparticles modified Au electrode for amperometric determination of uric acid, Appl. Biochem. Biotechnol., 174 (2014) 1683-1694.

[164] D. Jiang, C. Xu, Q. Zhang, Y. Ye, Y. Cai, K. Li, Y. Li, X. Huang, Y. Wang, In-situ preparation of lactate-sensing membrane for the noninvasive and wearable analysis of sweat, Biosens. Bioelectron., 210 (2022) 114303.

[165] G. Palleschi, M.H. Faridnia, Determination of lactate in human saliva with an electrochemical enzyme probe, Anal. Chim. Acta, 245 (1991) 151-157.

[166] H. Cheng, Volatile flavor compounds in yogurt: a review, Crit. Rev. Food Sci. Nutr., 50 (2010) 938-950.

[167] A. Londero, M.F. Hamet, G.L. De Antoni, G.L. Garrote, A.G. Abraham, Kefir grains as a starter for whey fermentation at different temperatures: chemical and microbiological characterisation, J. Dairy Res., 79 (2012) 262-271.